Disassociating Sensory, Choice, and Attentional Signals to Understand Feature Based Perception and Learning in Small Populations of Intermediate Visual Cortex

A DISSERTATION

SUBMITTED TO THE FACULTY OF THE

UNIVERSITY OF MINNESOTA

BY

Elisabeth Jayne Moore

IN PARTIAL FULFILLMENT OF THE REQUIREMENTS

FOR THE DEGREE OF

DOCTOR OF PHILOSOPHY

Adviser: Geoffrey M. Ghose

May 2019

Acknowledgements

This thesis was supported by National Institute of Health grants R01-EY014989, P30-NS057091, and R01-MH118487, as well as NSF grant DGE-1069104.

I would like to thank the entire Graduate program in Neuroscience (GPN) at the University of Minnesota, including my PI Geoffrey Ghose, my committee chair Matthew Johnson, and my committee members Stephen Engel, James Ashe, and Kendrick Kay, as well as James Ashe and David Redish as DGS during my time in the program, Linda McCloon as the aDGS, the GPN staff (John Paton, Elaine McCauley, Rebecca Hervonen), and the GPN class of 2013. I would also like to thank Peter Janssen and his lab members for skills I gained while completing an internship there.

Additionally, I would like to thank Katherine Weiner for data acquisition and analyses that laid the groundwork for the learning experiment, Kendrick Kay, Stephen Engel, and Scott Warren for their assistance in analyses and experimental design issues, Luca Vizioli and Andrea Grant, for assistance with fMRI data acquisition, Steve Schnell, Justin Aronson, Sean Moen, and Gregor Adriany, for their help with work with non-human primate training and/or experimental design issues, Ruyuan Zhang and others previously mentioned, for comments on drafts of manuscripts, as well as Katy Hagen and Matthew McHugh for their work on both of these projects as undergraduate researchers.

Abstract

Perception is integral to how we interact with our visual environment. How perception changes with experience is a function of learning, while how it occurs on a flexible, immediate time scale in relation to dynamic task demands, is mediated by attention. Both of these cognitive phenomena underpin how we perceive and interact with the world around us.

Visual perceptual learning (VPL) is the improvement in the ability to perceive our visual environment and is essential to how humans and other animals learn to interact with the world. Despite an extensive amount of research into the mechanisms of VPL, the neural mechanisms responsible for perceptual improvements remain controversial. A major challenge has been establishing that a particular physiological correlate of learning is actually responsible for learning, as opposed to merely reflecting changes in the properties or populations that are responsible. To address this issue, we employed a perceptual detection task in which neurons in a specific area, V4, are known to have task related responses on a scale of tens of milliseconds that reliably predict the timing and precision of shape detection. We followed population responses using a chronically implanted electrode array while non-human primates learned to detect shapes degraded by noise. Consistent with previous results that examined single neurons and neuronal ensembles, we found that, after the course of learning, variations in the local field potentials of individual electrodes over the course of tens of milliseconds reliably reflected the presentation of degraded shapes, and also predicted detection decisions made by the animal. Moreover, we found that variations in reliability of shape-related signals predicted the up-down fluctuations in performance seen over the course of learning in each animal. Together, these results demonstrate that population signals in area V4 are largely sufficient to explain the timing and reliability of shape detection and how that detection performance increases as a consequence of training.

Endogenous feature-based visual attention involves an improvement in neural representations involving the attended feature that is dependent on immediate task dependent demands. How this happens in a specific population, and whether the involved populations overlap with those mediating perception, is not well un-

derstood. Due to previous work in our laboratory finding that feature based attention is targeted to specific, task appropriate neural populations in early visual cortex (Warren et al., 2014), we asked whether attention is similarly distributed in a task specific way in V4, how this depends on attention state, and whether such neurons also signal the readout of the perceptual choice, given that choice signals have consistently been found in this area. We designed a demanding stimulus discrimination task where we directed subjects to attend to a specific feature of the task during high-field fMRI scanning. The stimulus alternated continuously at varying frequencies in low and high level features (spatial frequency and shape, due to their expected sensory activation of V1 and V4, respectively). Voxels were measured at high resolution, sampling 1mm of cortex, from V1 to V4, and the stimulus was presented near perceptual threshold in order to disassociate the stimulus from the choice. We used a linear regression analysis to compare continuous BOLD modulation of individual voxels to regressors modeling the continuous stimulus presentation when a given feature was attended to vs when it was not, and assessed how sensory and attention modulations overlapped with modulations containing a relationship to the ongoing perceptual choice. We found clear sensory attention effects in V4 that were specific to certain populations; however this did not appear to depend on initial sensitivity, and we did not see reliable choice signals or choice signals that overlapped with attention signals. We believe this may be due to the experimental design and recommend future approaches to disassociate sensory, attention, and choice signals in visual cortex.

Contents

List of Figures

1 Introduction

How we perceive the world is one of the most fundamental questions in cognitive neuroscience. A computer program can analyze an input and generate a reliable output that is a literal representation of the pixels, sounds, or other sensory inputs it receives. On the other hand, humans and other animals have an incredible ability to extract information from their environment that is an incomplete, non-literal view of the world but contains a flexibility that abstracts an enormous amount of biologically important information that even the most powerful computers cannot. This combination of flexible and non-linear, yet reliable, extraction of some information, while other irrelevant information is discarded, is the basis of perception. We do not see, hear, or feel every piece of information that enters our sensory organs. The brain determines which features are relevant to task demands on both short and long timescales, and processes such features from incoming sensory information, abstracting and processing such input into the mental percept that drives behavioral output.

Changes in how the brain processes sensory information must be responsible for task-dependent perceptual processing, and our extensive psychophysical and physiological knowledge of the visual system provides a promising basis for understanding these changes. The visual system can be precisely controlled with external stimuli, increases in visual performance with training are associated with changes in visual cortex, and the relationship between behavioral improvements and neuronal changes is quantifiable. Much has been elucidated about how the brain processes the pure stimulus information from a visual scene to form varying complexities of receptive fields (Lennie, 2003). Differences in light enter the retina and are separated by on and off cells in the lateral geniculate nucleus, which combine excitatory center fields with inhibitory surrounds to create orientation encoding in early areas such as V1, which then combine to form curvature and shape in higher areas such as V4, and then objects and faces in IT and beyond. However, what the human brain perceives is not equivalent to the pure sensory stimulus entering the retina, as would be expected from a simplistic interpretation of this hierarchical system. An expert in automobiles perceives far more details to

discriminate between types of cars than a non-expert; yet both the expert and layperson have the same exact visual stimulus input. Another example of perceptual complexity is a bistable stimulus, where a subject can perceive one of two objects, despite an unchanging stimulus. Additionally, performance during tasks improve if the subject is attending to a location or feature relevant to that task. Thus, learning and attention are integral in determining and changing what we perceive beyond simple stimulus processing.

1.1 Learning

How we learn to improve the accuracy of our perception, in order to perform various tasks, i.e. perceptual learning, is critical to understanding the dynamics of sensory perception. Perceptual learning is most simply defined as the increased ability to discriminate and detect sensory stimuli after experience. This type of learning is critical to interacting with our environment, whether learning to better detect and predict the movement of a ball when training in a sport (Abernethy et al., 2012), learning to detect and discriminate letters in reading (Chung et al., 2004; Nazir et al., 2004), or learning to differentiate familiar individuals on the basis of facial information (Burton et al., 1999; Ritchie and Burton, 2016).

Perceptual learning is a fundamental process that occurs throughout adulthood, allows us to learn from past experiences, and more efficiently perform perceptual tasks. Yet, while many studies have utilized the visual system to understand perceptual learning, due to its extensive baseline characterization, and found neuronal correlates of visual perceptual learning (VPL), the nature and locus of the cortical changes actually responsible for behavioral improvements remains controversial (Sasaki et al., 2010; Sagi, 2011; Shibata et al., 2014). It has been difficult to identify at which level in the brain VPL occurs, how neurons within a region are differentially altered to improve performance, whether signaling in various regions causes behavioral improvement, or only reflects changes elsewhere, as well as under what conditions learning is specific or can generalize to other contexts/features. Although the visual system has the advantage of controlled, external stimuli, it is still highly complex and comprised of multiple brain regions that receive both bottom-up and

top-down inputs. Where and how visual perceptual learning (VPL) improvements are mediated within the vast networks of visual areas is not readily apparent.

1.1.1 VPL as Encoding (Early) or Decoding (Late) Changes

Whether VPL is mediated by changes at early or late levels asks a fundamental question about how the brain codes for perceptual changes. If sensory representations change with learning, it is the brain's encoding that is altered, whereas if higher level areas change to better read out encoded representations, then this is more an issue of changing how the brain decodes existing, immutable representations. More than likely, some combination of these possibilities occurs, as the wide variety, of results and proposed, yet incomplete, models, implies.

Early psychophysical studies of VPL revealed training effects that were often specific to low-level features of the trained stimulus, such as location, orientation, and even eye (Karni and Sagi, 1991; Ahissar and Hochstein, 1993; Schoups et al., 1995), which suggested that the locus of such learning was in early visual areas, in which such features are segregated between different neural populations (Fahle, 2004). Even training the same task at several locations can induce specificity for the trained locations compared to untrained locations only a couple of degrees away (Le Dantec and Seitz, 2012), and VPL changes in human electroencephalogram (EEG) signals also suggests early changes (Bao et al., 2010). Further support, for the hypothesis that changes in early areas are responsible for learning, came from studies that found that attention and training were not always necessary for VPL, and that passive stimuli can result in behavioral changes (Watanabe et al., 2001). If simply being exposed to a stimulus can induce learning, without any involvement of higher level cognitive features, this suggests that changes in early visual areas may be sufficient for learning.

However, other studies and proposed models have implicated higher level areas and the involvement of top down processes (Ahissar and Hochstein, 2004; Law and Gold, 2008; Law and Gold, 2010; Zhang et al., 2010b), with more recent experiments demonstrating that VPL in fact can be more generalized and that the specificity of VPL reported in such studies may be dependent on the task and training designs employed (Xiao

et al., 2008; Wang et al., 2012; Zhang et al., 2010c; Hung and Seitz, 2014; Xie and Yu, 2018). Several such studies explored double training paradigms, where task-irrelevant features were included in the perceptual training, and this resulted in learning that transferred to the task-irrelevant features (Xiao et al., 2008), with thresholds equal to that of the trained location (Xie and Yu, 2018). This result, that learning could occur for features present but not relevant during a task, implicated the involvement of top down, less retinotopic, cortical sites. If learning related changes affected general features of a stimulus, learning must be at least partially mediated by less retinotopic, stimulus specific areas than early visual cortex. Additionally, one group has found that a stimulus may not even be necessary for VPL and that imagery alone is sufficient (Tartaglia et al., 2009; Tartaglia et al., 2012). Given that mental imagery requires an intentional creation of an abstraction of an image that is not actually stimulating the visual system, these results makes it difficult to argue that early visual areas are causally involved in, or at least necessary, for learning. Additionally, attention, which is well established to involve higher areas, also increases the information contained in V1 neurons during VPL (Li et al., 2004). VPL transfer between overlapping but different types of VPL tasks has also been observed (McGovern et al., 2012). These results all strongly challenge the hypothesis that early, stimulus-specific areas like V1 are mediating the bulk of VPL changes, and suggest that higher level areas that mediate attention and mental imagery are more likely to be critical.

Variations in task and training may also explain the diversity of results in the physiological literature, which is similarly contradictory to psychophysical results. Early areas such as V1 are highly retinotopic, with specific sets of neurons representing not only specific orientations (horizontal, vertical, etc.), but also only responding if the stimulus is in a specific location of the visual field (known as a ”receptive field”). Thus, if changes in the encoding in such areas mediate learning, not only should behavioral results be specific to the trained orientation and location, but physiology studies should find that only the populations tuned to the trained orientation/location improve, as well as that this is related to the perceptual decision. Some studies have found that changes in early visual areas, such as V1, occur with training. For example, V1 neurons were

found to change if they were tuned to the trained orientation of a stimulus, using electrophysiological recordings (Schoups et al., 2001), fMRI (Engel et al., 2004; Jehee et al., 2012), and two photon microscopy (Poort et al., 2015). Another study found that not only were neurons tuned to the trained stimulus strengthened, but also that neurons responding to the training-irrelevant background of the stimulus were suppressed (Yan et al., 2014). However, other studies have found the opposite, that neural properties in V1 were immutable (Ghose et al., 2002), where there were no changes in the populations tuned to the trained orientation and location. Similarly, many have found that when early changes are present, they are irrelevant to, or cannot account for (Palmer et al., 2007), behavior or the stimulus (Choe et al., 2014). Another study found that choice probabilities increase in V2, but not V1, after training (Nienborg and Cumming, 2006). Early changes might only represent feedback from other brain regions, which is supported by a finding that choice probabilities, when they did exist, were negatively correlated with behavior in both V1 and V2 and most likely represented modulation after the decision (Goris et al., 2017).

There have been attempts to combine these contradictory findings into one model that explains the competing observations of specific, early neural changes vs generalized, high level late changes, including by framing VPL as an interaction of feedforward and feedback mechanisms (Bejjanki et al., 2011; Li, 2016). Some models separate VPL into two different types (Watanabe and Sasaki, 2015), propose that VPL is mediated by re-weighting early sensory representations via higher level areas (Dosher and Lu, 1998; Dosher and Lu, 1999; Petrov et al., 2005; Talluri et al., 2015; Sotiropoulos et al., 2018), or postulate that task difficulty or precision could play a role in variations in specificity (Ahissar and Hochstein, 1997; Jeter et al., 2009; Wenliang and Seitz, 2018). However, despite the plethora of proposed models, there is no consensus within the field that reconciles the seemingly contradictory findings.

One possible explanation for this controversy lies in the highly interconnected nature of visual processing in the cerebral cortex. Given the pervasiveness of feedforward, feedback, and lateral connectivity within the multiple areas associated with vision, sensory signals that are not directly responsible for perceptual

performance, in an addition to those that are, may change with VPL. Behaviorally, this can be seen in experiments where subjects improve in sensitivity to low level features that do not obviously seem relevant to performance in the trained task. For example, several papers have found that expert video game players have improved contrast discrimination (Sowden et al., 2000; Li et al., 2009) and reading performance (Nazir et al., 2004), compared to non-experts, and functional connectivity changes have also been observed with learning (Baldassarre et al., 2012; Sarabi et al., 2018). A critical prerequisite, for establishing whether changes in a neural population are responsible for improvements in the performance of a perceptual task, is therefore to establish that the population actually plays a role in the performance of that task. Physiologically, the task relevance of sensory neurons has been addressed by looking for neurons whose firing both reflects the stimulus and, in difficult tasks based on that stimulus, predicts behavioral choices. For example, if, in a detection task, a neuron reliably signals a stimulus, but has no relationship to whether or not the animal reports the stimulus, then it cannot be causally involved in detection and therefore not associated with any improvements in detection that arise through training (Parker and Newsome, 1998). On the other hand, if sensory responses are predictive of choices, it suggests the possibility that such neurons contribute in a feedforward manner to perceptual decisions (Zuo et al., 2015; Panzeri et al., 2017). In the neurons in such a brain region, learning could arise from more selective or reliable encoding of sensory responses, and thus changes in low level representations at or preceding the area of interest. Conversely, learning could be mediated by a stronger relationship of sensory responses to behavioral choices, where the decoding, i.e. readout (Nienborg and Cumming, 2009), of sensory representations by areas at or above the given brain region, improves to mediate learning. Some combination of improvements in encoding and decoding could occur as well. Moreover, changes in either of these properties should correspond to the behavioral time course of learning (Yan et al., 2014). Yet, to date there have been no studies which follow sensory and choice related signals in the same neural population during the process of training to examine their potential to explain task performance on a moment to moment basis, and how that

performance changes with learning over the course of many days.

1.1.2 Methodological Concerns

Identifying the locus of VPL has also been challenging because traditional electrophysiological analyses cannot readily separate sensory and choice contributions to neural activity, and thus the two phenomena have often been conflated. Many studies (Law and Gold, 2008; Sanayei et al., 2018) have used neural sensitivity and choice probability measures. However, sensitivity and choice probability do not correct for covariance between the stimulus and the behavioral decision, and this potentially conflates stimulus and choice, complicating interpretations. Stimulus-related responses have been found to determine the amplitude of choice probability (Kumano and Uka, 2013) and, because of neuronal correlations, choice probability need not reflect the feedforward influence of a neuron upon behavior (Nienborg and Cumming, 2006; Cohen and Newsome, 2009; Nienborg and Cumming, 2009; Churchland et al., 2010; Zaidel et al., 2017). Additionally, standard trial averaging of stimulus and choice aligned responses, given the interactions between sensory and choice related signals, especially within the narrow time window that defines rapid detection, makes it difficult to isolate these signals through such analyses (Panzeri et al., 2017). An additional challenge of such analyses is that, by averaging over all electrodes and all trials, the moment to moment ability of signals among small neural populations to signal the shape and predict the saccade is still unknown. These challenges can be addressed, however, by adopting a moment-to-moment mutual information approach which avoid such averages and can make use of a covariance correction to isolate sensory and choice signals (Harrison et al., 2013) (see Experiment 1: methods section).

Another issue in studying VPL, is that learning has often been described monotonically, assuming that early and late periods adequately represent learning effects. However, in reality, learning often contains ups and downs as a subject adjusts strategies and processes new information, especially when tasks contain noise and uncertainty (Gureckis and Love, 2009). It is a fundamental concept in sensory perception that if a neuron is involved in sensory perception, fluctuations in this neuron's signals should have perceptual consequences

that can be measured behaviorally (Parker and Newsome, 1998). Yet this basic principle has usually not been applied in the context of long term perceptual learning, due to the experimental challenges of measuring neural responses in a given population over the course of days or weeks or training. If neural populations are truly involved in and causing learning related changes, they should not only improve in their sensory representations and/or choice predictions in late compared to early periods, but those measures should also track the ups and downs of the behavioral learning process. This has been done on a day to day basis in V1 (Yan et al., 2014), but given that individual training days may vary in number of trials and stimulus presentations, a point to point, moving average process may more accurately represent fluctuations over time. While, to our knowledge, the relationship between behavioral fluctuations during VPL and neural signals has not been studied in this way, this is a critical piece to inferring involvement of specific neural populations and behavioral changes. We address this by looking at equal bins of trials across weeks of training (see Experiment 1: methods section).

1.1.3 Local Field Potentials

Past work studying the neuronal correlates of VPL has also often depended on either spike analyses from single, and occasionally multi-, units, in macaques (Ghose et al., 2002; Yang and Maunsell, 2004; Rainer et al., 2004; Raiguel et al., 2006; Palmer et al., 2007; Adab and Vogels, 2011; Shiozaki et al., 2012), or fMRI in humans (Engel et al., 2004; Kourtzi et al., 2005; Zhang et al., 2010a; Byers and Serences, 2014; Choe et al., 2014; Sarabi et al., 2018). However, single unit analyses are limited in spatial coverage, while fMRI is limited in temporal resolution, making it difficult to link signals in small populations to perceptual decisions, and changes in signals over time, that must occur over millisecond timescales. This disparity has also made it difficult to compare macaque and human VPL literature. However, we may be able to bridge these gaps by analyzing local field potentials (LFPs). To our knowledge, LFPs have not been previously utilized in VPL studies, yet there is evidence that they may more closely represent the results from BOLD signals than single and multi unit activity, in a near linear manner (Logothetis et al., 2001; Goense and Logothetis, 2008), and

that cortical LFPs can also be related to, and predict, spike trains (Rasch et al., 2008; Manning et al., 2009; Denker et al., 2011). LFPs have also shown promise in understanding stimulus representations (Belitski et al., 2008; Montemurro et al., 2008) and complex perceptual and cognitive features (Wang et al., 2009; Rey et al., 2015), both alone (Lopour et al., 2013) and in combination with spikes (Rutishauser et al., 2010).

Despite the potential for LFPs to reveal more than spikes, they have often been avoided in electrophysiology analyses, as what LFPs sample and how far they spread is controversial. They contain both sub- and supra-threshold spike activity, as well as non-synaptic activity (Buzsáki et al., 2012). While some studies have suggested relatively fixed, small spatial sampling (Xing et al., 2009; Katzner et al., 2009), others have found that spread can be larger and more complex (Kajikawa and Schroeder, 2011; Kajikawa and Schroeder, 2014). It has also been found that they reveal information from multiple spatial scales in V4, with smaller spatial information ($\approx$ 350 μm) dominating early components of the signal (Mineault et al., 2013). Thus, in the case of moment to moment analyses on millisecond timescales, like we employ, LFPs are likely sampling smaller spatial scales. Additionally, despite LFPs pooling a large number of neurons, some models demonstrate that informative signals in a pool of noisy neurons can dominate signals (Krause and Ghose, 2018), allowing us to extract information from a small number of informative neurons contributing to the LFP signal, as noisy signals cancel each other out, particularly in the absence of strong noise correlations. We utilize LFP signals for these reasons.

1.1.4 Neuronal Correlations and VPL

Correlations between neurons and populations also potentially play a role in learning. Stimulus input alone induces decreased variability across cortex (Churchland et al., 2010), and reduced noise correlations have been found after learning in MSTd (Gu et al., 2011; Sanayei et al., 2018) and V4 (Ni et al., 2018). However, a lack of noise correlation changes were observed in V1 (Yan et al., 2014; Ni et al., 2018), and measurements of V4 ensembles during shape detection have revealed that such correlations are largely absent (Weiner and Ghose, 2015). Learning studies of modalities besides vision has also found that learning may

increase population coding through decreased noise correlations, in a stimulus specific way, particularly in pools of neurons (Jeanne et al., 2013). Thus, understanding the relationships between populations may also be important in elucidating the mechanisms of VPL.

1.2 Attention

Attention is another powerful phenomenon that alters visual perception. While learning improves performance on a task based on experience and relevance, attention improves performance based on short term behavioral relevance. Yet the two can also interact (Byers and Serences, 2012). Just as we must select which information is behaviorally important to learn, we must also select what is most important to attend to in the short term. While sports players may learn to better perceive the movement of a ball over weeks or months of training, they must also anticipate where the ball is likely to appear in a short time span of hundreds of milliseconds and attend to that area, to the exclusion of others. We cannot possibly process every piece of information coming into the visual system and behave effectively on short timescales; attention solves this problem by selecting only that which is determined to be relevant to behavior. In this way, the behavioral response to two identical stimuli can vary, based on the goal at hand.

This enhanced focus, on a specific portion or attribute of a visual stimulus, improves performance on detection and discriminability of visual tasks, even without prior experience/learning. Sensitivity to the attended attribute of the stimulus is increased (Yeshurun and Carrasco, 1998) and reaction times for behavior is decreased (Posner and Cohen, 1984). This phenomenon ultimately leads to perceptual alterations of both low and high level features (Carrasco and Barbot, 2019), such as contrast (Carrasco et al., 2004), spatial frequency (Gobell and Carrasco, 2005) and object size (Kirsch et al., 2018). Attention is a broad term however; it can be overt or covert, with the latter referring to attending to an object peripherally without a saccade (eye movement). It can also be exogenous (involuntary) or endogenous (voluntary), with the latter being more delayed (Liu et al., 2007; Carrasco, 2011). Additionally, attention can be directed to a particular spatial loca-

tion or feature, and covert attention improves spatial resolution in the area attended (Y and M, 1999). For the purpose of this thesis, we focus on covert, endogenous attention, because we are interested in how perceptual choices relate to attention. Are the mechanisms, driving the effects of endogenous attention on perception, similar to, or overlap with those of learning? Is attention a large scale, general effect, or is it targeted to specific, task relevant populations? If we methodically disassociate the relationships between neural signals and sensory, attention, and choice conditions, are the visual neurons that encode the perception (i.e. choice) more modulated by attention than neurons that are unaffected by attention, and how do both attention and choice relate to initial sensitivity to a stimulus in a demanding attention task?

1.2.1 Global Effects

Some studies have found that attention appears to be very generalized. While modulation occurs in early visual areas, many results suggest that such changes appear to be mediated by top-down feedback that create a multiplicative gain effect on neural sensitivity. Feature based attention increases activity throughout the visual system (Saenz et al., 2002), and attention also not only improves responses to the attended feature at the task location, such as motion, (Carrasco, 2011), but unlike exogenous attention, performance improvements also transfer to the attended feature at unattended locations (Arman et al., 2006; Bartsch et al., 2018), across all eccentricities (Yeshurun et al., 2008). This lack of location specificity implicates flexible top down, non-specific mechanisms in higher brain regions. Transfer occurs to locations that are not ever visually stimulated, implying a global, baseline effect (Liu and Mance, 2011), and spatial attention can generalize across modalities, resulting in physiological activation in frontoparietal regions, regardless of whether attention is visual or auditory (Zuanazzi and Noppeney, 2019). Additional support comes from studies finding that neuronal discriminability changes with attention in a way that can explain performance in higher level areas like LIP, but not earlier areas such as V4 (Arcizet et al., 2018).

1.2.2 Flexible/Specific Mechanisms

However, while higher brain regions and feedback are undeniably important in attentional modulations, such feedback may be more specific than originally suspected. To some extent this must be true, in order to explain the specific behavioral improvements mediated by attention. What we need to pay attention to is essentially limitless; it would be hard to argue that a global increase alone could differentiate the wide array of possible simple and complex attributes that we can attend to within a visual scene. While a global baseline increase does occur, attention also alters the relationship between behavior and neural signals variably across visual areas (Maunsell and Cook, 2002), and in specific task conditions, may be selectively mediated by high frequency filters that can flexibly enhance or decrement resolution to improve performance (Barbot and Carrasco, 2017), depending on the behavioral goal (Anton-Erxleben and Carrasco, 2013). Attention has also been found to increase perception in accordance with changes in early sensory areas (Störmer et al., 2009), and baseline increases may be more related to location than feature attributes (McMains et al., 2007). Additionally, biased competition experiments (Moran and Desimone, 1985) have demonstrated that if a preferred and non-preferred stimulus orientation are simultaneously presented within a V4 neuron's spatial receptive field, an intermediate response will occur, but if either stimuli is attended, the neuron will increase or decrease, if the attended stimulus is of the preferred or non-preferred orientation, respectively. This suggests that attention is acting at a highly specific level in order to select the appropriate stimulus and enhance processing of the neurons tuned to the attended stimulus. This could lead to the conclusion that attention may act on an individual cellular level, and indeed, changes in selectivity do occur, allowing for a dynamic, task dependent improvement in sensory representations that alter perception, enhancing the spatial resolution of stimuli at the locus of attention (Cutzu and Tsotsos, 2003; Anton-Erxleben and Carrasco, 2013). Some studies have also suggested that attention can alter receptive field (RF) sizes in highly specific ways, by shrinking the RF at the locus of attention, expanding nearby RFs, shifting both the center and surround of the RF in the direction of the attended location (Anton-Erxleben

et al., 2009), and even changing receptive fields at different levels of the visual system based on the size of the attended stimulus, within a few hundred milliseconds, even when the scale cannot be anticipated by the subject (Hopf, 2006). However, this is controversial, as other studies have found that there is no change in the receptive field structures of individual neurons.

Expectation in conjunction with attention also creates non-linear modulation specific to certain receptive fields, and this cannot be explained by a global gain increase alone (Ghose and Bearl, 2010). Pre-saccadic shifts are another mechanism by which RFs are specifically altered to improve performance via a focus on the immediate goal at hand (Sun and Goldberg, 2016; Binda and Morrone, 2018), where RFs have been found to change their tuning to the location at the center of the future saccade, a few hundred milliseconds before the saccade. Given the intertwining of endogenous visual attention and saccades, it stands to reason that the mechanisms of pre-saccadic shifts and attention may overlap. Two types of pre-saccadic RF mapping have been found to occur: future field (FF) remapping towards the location to be occupied after the saccade, and saccade target (ST) remapping towards the saccade target regardless of the RF to be occupied after the saccade (Neupane et al., 2016a; Neupane et al., 2016a). Both appear to occur in area V4 (Neupane et al., 2016b). While FF remapping appears to occur in order to modulate perceptual stability (Neupane et al., 2016a), ST is more likely an attentional mechanism, with the latter occurring later than the former, and this effect can be seen in both single neurons and LFPs (Neupane et al., 2016b). Since both are predictive, they must involve the influence of feedback from higher brain regions, especially considering that remapping effects, in higher regions such as FEF (Joiner et al., 2011) and LIP (Gottlieb et al., 1998), are small for unattended stimuli but large for attended/salient stimuli. Remapping has particularly been found to occur in order to modulate and stabilize attention in area V4, where RFs shift in a predictive manner based on the future focus of attention (Marino and Mazer, 2018). Thus, non-linear effects mediated by top down feedback, due to changes in cognitive states such as attention, do clearly exist. A remaining question, however, is at what neural resolution this occurs.

While there clearly are synaptic level effects of attention, these do not appear to be non-linear; but rather multiplicative and gain-like (Motter, 1993). Therefore, gain modulation may affect neurons, while non-linear task specific effects occur in larger pools of neurons. Our lab has found support for this; non-spatial attention in V1 modulates populations of neurons tuned to the attended feature, temporally matching the attention-related behavior (Warren et al., 2014). The non-linear effects of biased competition in V4 were also found to be explained by pooled population effects in early visual cortex that contribute to downstream neural inputs (Ghose and Maunsell, 2008; Ghose, 2009). It may be that specific effects that change the structure of signaling, in the targeted ways necessary to mediate precise behavioral effects, may occur at a larger scale than individual neurons. Given that we have also found that populations of neurons are more reliable at predicting behavioral changes with learning (see Chapter 1), this may also be the case for attention, where specific, early changes in pools of neurons may be important in mediating the effect of attention on perceptual behavior.

1.2.3 Attention and Neuronal Correlations

Another argument for the importance of small neural populations in non-linear attention effects, is that like learning, attention may also mediate changes in behavior by decreasing noise correlations between neurons (Cohen and Maunsell, 2009; Cohen and Newsome, 2009). One model (Kanashiro et al., 2017) proposes that attention can be understood as changes in correlations that occur via shared and private recurrent excitatory-inhibitory connections in local populations (specifically V4) that are also influenced by top down attentional modulation. Top down modulation may decrease variability via inhibitory feedback to recurrent connections, while canonical gain enhancements may be due to increases in excitatory firing, and stimulus response gains mediated by enhanced sensitivity of excitatory neurons to feedforward stimulus inputs that are increased by attentional modulation. Thus, it does appear that the interactions between populations, at a larger scale than individual neurons, may be important in understanding the effects of attention. Additionally, correlations in spiking between brain regions (such as V1 and MT) are increased by attention (Ruff

and Cohen, 2016); thus, changes in both late and early brain regions may best explain behavioral changes with attention. Changes in correlations have also been proposed to link perceptual learning and attention, as decreases in trial to trial variance and pairwise correlations explain behavior in both short term attention and long term perceptual learning tasks in V4, but not V1 (Ni et al., 2018). However, neuronal correlations also highlight the difficulties of separating sensory and choice effects and determining if signals are due to attention or feedforward sensory inputs, as changes in the structure of correlations with feature based attention can create choice probabilities (Cumming and Nienborg, 2016). Thus it is imperative, when studying populations, to ensure that the effects are measured and analyzed in ways that allow for a distinction between between sensory, attention, and choice effects.

1.2.4 Attention and Choice

If attention alters perception, then it should also have an effect on behavioral choices, and it follows that neurons that are modulated by attention may also be modulated by perceptual choice. Previous work from our lab has found that the reliability of neurons in MT decreases substantially when a stimulus is unexpected, and thus unattended, and this matches with decreases in behavioral choices (Harrison et al., 2013). However, disassociating attentional signals from choice signals is difficult, especially in regards to studying neural populations, for similar reasons as it is in regards to perceptual learning. Thus, it is necessary to select an experimental design that can disassociate the sensory/attention signal from the choice signal. One potential approach is to separate the stimulus from the perception, and thus the perceptual report, in time, with a task that is very difficult, where both the stimulus and the perceptual report fluctuate in a non-binary way over time. In this way, the perceptual report/choice is distinct in its fluctuations from the stimulus, and a signal from given brain regions can be regressed against the stimulus or choice fluctuations. Ultimately, this may address the question of whether specific, small populations in early and/or intermediate visual cortex can explain variation in attentional state, and if so, whether such signals co-vary with signals that can explain the behavioral choice.

1.3 V4: Linking Learning and Attention

As with learning, area V4 is a particular area of interest in understanding the intersection of attention and perception. Given the frequent lack of learning signatures in early visual cortex (V1), we plan to focus on this particular visual area, which has been implicated in intermediate visual processing (Kobatake and Tanaka, 1994; Pasupathy and Connor, 2001; Carlson et al., 2011; Roe et al., 2012; Kosai et al., 2014), attention (Neupane et al., 2016b; Neupane et al., 2016a; Marino and Mazer, 2018), and learning (Yang and Maunsell, 2004; Rainer et al., 2004; Raiguel et al., 2006; Adab and Vogels, 2011; Shiozaki et al., 2012; Sanayei et al., 2018). Meanwhile, stimuli activating the receptive fields in this area are not too complex to be experimentally controlled; V4 is known to be responsive to curvature and shape (Pasupathy and Connor, 2001), as well as natural textures (Arcizet et al., 2008). Thus V4 is an ideal target for stimuli that are more similar to natural stimuli but still controllable in a rigorous way. V4 is also an integrative area that is responsive to perceptual features not necessarily contained in the stimulus, given that this area is responsive to illusory contours (Cox et al., 2013). Both spatial and feature based attention also occur in area V4 (McAdams and Maunsell, 2000), and feature based attention has been found to shift the tuning of V4 neurons based on the attended stimulus (David et al., 2008). Previous work in our lab has also linked sensory and choice signals in V4 in both single units (Weiner and Ghose, 2014) and populations (Weiner and Ghose, 2015). Given this apparent relationship of neural signals to perception, attention, and learning in area V4, we mainly focus on this area to understand the intersection, overlap, and specificity of sensory and choice signals, using shape stimuli to activate V4 sensory neurons, in both our attention and learning studies. Also, in order to understand the population effects of perceptual changes in both humans and macaques, we use BOLD signals in our attention experiment, given their apparent similarity to LFPs (Logothetis et al., 2001), which we use to study VPL in macaques (see Learning introduction). While ideally we could use both signals and both species in both experiments, this is a first step in studying population effects in both animals in both short and long term perceptual changes (attention and VPL, respectively).

1.4 Relevance

Attention and learning are integral to how perception changes, and alterations to perception underlie a variety of disorders. Understanding the fundamental signalling mechanisms of attention and learning is essential to understanding how perception affects behavior both in healthy and disease states. We expect our findings regarding VPL to be relevant to understanding multiple diseases, including visual disorders such as amblyopia. Learning generalizability is increased in amblyopic patients, and VPL training is effective in treating amblyopia and other visual disorders (Huang et al., 2008; Shibata et al., 2014). This work may also be applicable to schizophrenia, where generalization of memories and application to novel experiences has been found to be impaired (Shohamy et al., 2010). Understanding perceptual learning may also be integral in developing effective teaching strategies. Students improve in performance on declarative equation solving tasks when perceptual learning training is administered simultaneously, compared to those receiving declarative only instruction (Kellman et al., 2010), for example. Additionally, attention is important in understanding every day functioning, as well as disorders where attention is impaired, such as attention deficit disorder (Epstein et al., 1997), autism (Gadgil et al., 2013; Robertson et al., 2013), and Alzheimer's disease (Greenwood et al., 1997). Therapies involving attention training have shown physiological (Beauregard and Lévesque, 2006) promise in treatment, although more work is needed to establish how clinicians might maximize behavioral effects (Cortese et al., 2015). Visual attention training has also shown promise in treating attention deficits found in schizophrenia (Medalia et al., 1998), and both attention and perceptual training may improve problems with attention after strokes (Mazer et al., 2003). Thus, deciphering the underlying neural substrates mediating, and the overlap between, visual attention and visual perceptual learning, may ultimately allow us to understand how to solve problems, diseases, and deficits in such neural systems, and improve perceptual therapies targeting visual attention and learning.

2 Experiment 1: Population level shape detection signals in area V4 explain the magnitude and dynamics of perceptual learning

2.1 Introduction

To address whether changes in encoding or readout mediate VPL, we leveraged recent observations from our laboratory, which found that neurons in area V4 carry reliable sensory and choice related signals that are consistent with the latency and temporal precision of rapid shape detection (Weiner and Ghose, 2014; Weiner and Ghose, 2015). To examine the role of such neurons in perceptual learning, we recorded LFPs across a chronically implanted microelectrode array while monkeys learned to detect degraded shapes over the course of several weeks. We analyzed these recordings across two time scales. On a time scale of milliseconds, we found that, after training, LFPs on single electrodes reliably reflected both degraded shape presentation and predicted detection of those shapes, suggesting that they contributed in a feedforward manner to shape detections. In contrast to the results obtained from smaller V4 populations, we found that the signals on particular electrodes were largely sufficient to explain both the timing and reliability of shape detection. Moreover, on a time scale of hours, we found that the reliability of low latency shape signals, reflecting stimulus encoding at level of V4 or earlier, closely tracked fluctuations in performance during the course of training. Together, these results demonstrate that local population signals in area V4 are largely sufficient to explain the timing and reliability of shape detection, and how that detection improves with training.

2.2 Materials and Methods

2.2.1 Ethics Statement and Surgical Procedures

All procedures involving animals conformed to guidelines established by the National Institutes of Health and were approved by the Institutional Animal Care and Use Committee of the University of Minnesota. Animals were initially anesthetized with ketamine, and anesthesia was maintained with isoflurane throughout

all surgical procedures. Analgesics and antibiotics were administered during and following all surgeries to minimize discomfort and prevent infection. To stabilize head position during training and recording sessions, headposts (PEEK polymer) were chronically implanted under sterile surgical conditions. Animals were fully acclimated to their primate chair and training room before headposts were used for stabilization. Once each animal was trained on the shape detection task, a 96-element microelectrode ("Utah") array was chronically implanted, again under sterile conditions.

2.2.2 Task and Training

Two experimentally naive subjects (*Macaca mulatta*), Monkey Z and Monkey J ($\approx$ 7 and 13kg), were trained to saccade to a shape. During the task, the subjects' head position was stabilized by a chronically implanted headpost. Eye position was monitored by an infrared eye tracker (Arrington Research). Subjects viewed the stimulus on an LCD monitor (120 Hz), and a photodiode attached to the screen confirmed the timing of stimulus presentation. The stimulus consisted of a 7x7 array of achromatic Gabors, the appearance of which was controlled by a custom software program (http://www.ghoselab.cmrr.umn.edu/software.html). The stimulus overlapped the receptive fields covered by the microelectrode array (an eccentricity of 3.75° - azimuth: 3.75°, elevation: 0.2° for Monkey Z; and an eccentricity of 5.5° - azimuth: -2.5°, elevation: -4° for Monkey J). The size of each Gabor was 0.38 °; receptive fields thus covered 16-25 Gabor elements (Motter, 2009; Gattass et al., 2014). Gabors had a spatial frequency of 2 cycles/°.

Visual Stimulation Noise stimuli in the Gabor array were set to one of eight random orientations, independently for each Gabor. To eliminate motion cues as a potential confound for contour detection, the noise stimulus was constructed by interleaving two types of these noise frames among frame updates: static and redrawn. A single static noise frame was generated at the beginning of each trial, but was not varied within a trial, such that the pattern was consistent between alternate frames. In between these frames, a new random pattern was generated, such that this pattern varied between successive presentations. Our frame rate of 120 Hz meant that each static/redrawn frame was present for 8.3 ms. During shape presentation, the Gabors defin-

ing the shape replaced the corresponding Gabors within the static noise frame, but this combined static-shape frame continued to be interleaved with randomly redrawn noise frames. The shape to be detected ("Pacman") was defined by fixing the orientations of 16–19 adjoining Gabor patches so as to form a contiguous contour. During recording sessions, the Gabor elements of both the shape and noise appeared at the same contrast (45 – 50%).

Task A trial began with the appearance of a fixation dot (0.1°), which the subject was required to continuously fixate on, within a fixation window ($< 3°$), before and during the appearance of the stimulus. If the animal made eye movements outside of this window when the shape was not present, the trial would instantly abort without reward. Once the fixation dot appeared, and fixation began, a noise stimulus consisting of randomly oriented Gabors appeared after a delay of 500 ms. Animals were required to maintain fixation during this noise, and saccade to the location of the visual stimulus only following a brief shape stimulus (83ms for Monkey Z or 120ms for Monkey J) presentation. Saccades were defined by the beginning of the time that the animal left the fixation window. Animals were rewarded with juice for making this saccade within a reaction time window (150-550 ms), which ensured vigilance. The timing of shape appearance relative to the start of the noise was exponentially distributed and random so that the subject could not predict when it would appear (Ghose, 2006). "Catch" trials, in which no shape stimulus event appeared and the subject was rewarded for maintaining fixation throughout the entire trial, were also included 5% of the time.

Implantation Once the subjects could perform this shape detection task, we implanted a chronic 10x10 microelectrode array in visual area V4 on the prelunate gyrus (Monkey Z: left hemisphere, Monkey J: right hemisphere), slightly above the tip of the interior occipital sulcus. The array was 4-mm in length with 400- μM spacing, and was injected with a 1-mm pneumatic inserter (Blackrock Micosystems). Local field potentials were recorded during task performance.

Task Training Period After implantation, subjects performed the task during the "pre-training" period. Data from this pre-training period are not reported in this study but were reported previously (Weiner and

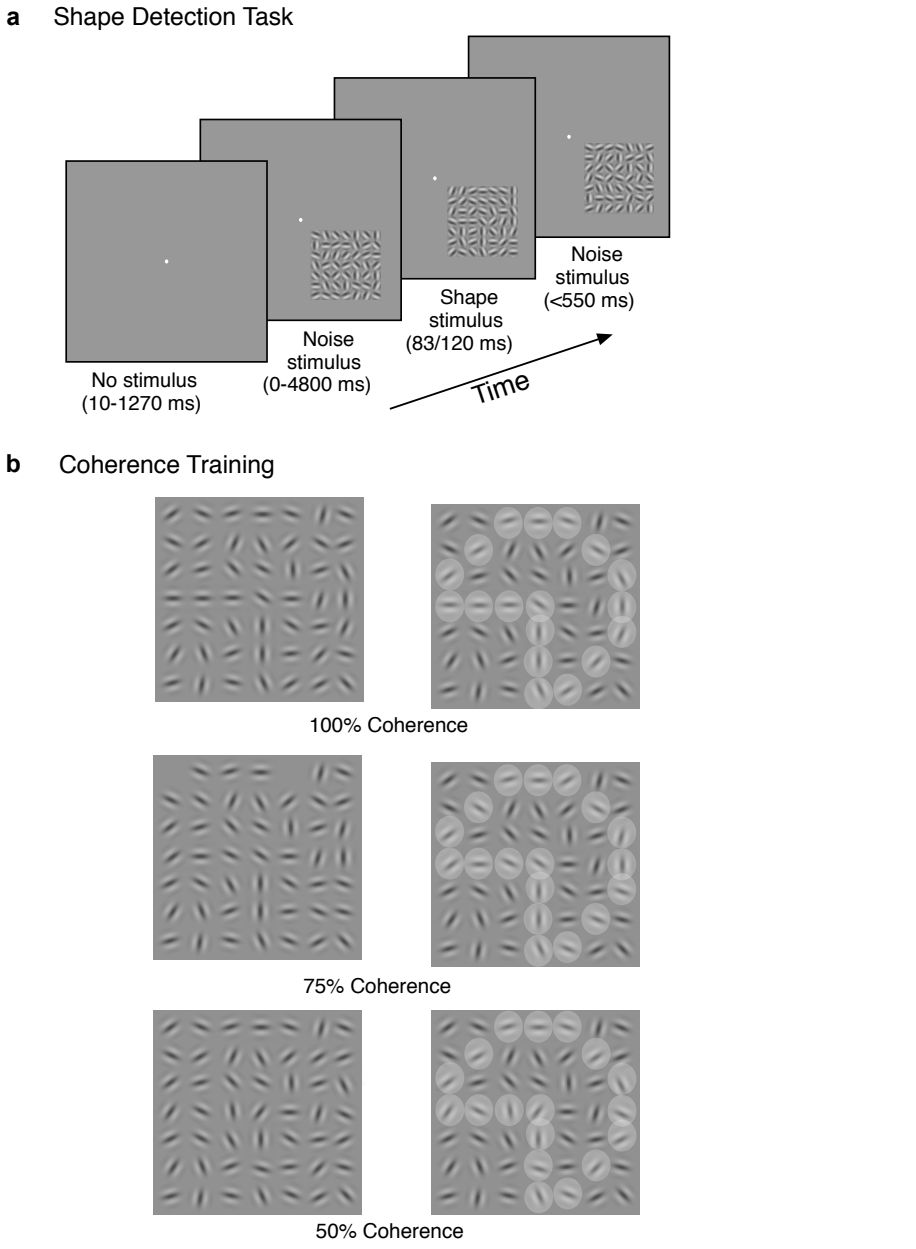

Figure 1: Learning Task: a.) A fixation dot followed by a background of randomly oriented Gabors (noise stimulus) appeared before the shape stimulus. The shape (”Pacman”), defined by colinear Gabors embedded within the noise stimulus, briefly appeared (83ms for Monkey Z or 120ms for Monkey J). The noise stimulus then returned for the duration of the trial, which aborted once the monkey saccaded or failed to saccade within the allowable reaction time window (150-550ms). b.) Once subjects had learned the task with a fully colinear stimulus (100% coherence), they underwent a coherence training protocol, where the shape was degraded, where a given percentage of the colinear Gabors were selected to be randomly oriented. Left stimuli are shown as presented to the subject; right stimuli show the Gabors, that are in the outline of the shape, as highlighted.

Ghose, 2014; Weiner and Ghose, 2015). In this period, the subjects performed a shape detection task using multiple different shapes. Then, over a period of 30 days for Monkey Z, and 28 days for Monkey J, the task was slowly biased to only contain Pacman shapes. Correct reports of the shape during this time period was ≈40% (Weiner and Ghose, 2014), indicating the task was challenging even during the pre-training stage.

Perceptual Learning Period After the pre-training period, we degraded the spatial coherence of the Pacman shape on some trials (Figure 1b), where spatial coherence is defined by the colinearity of Gabor elements forming the shape. Degraded stimuli could have values of 87.5%, 75%, 62.5%, or 50% of the fully coherent (100%) Pacman shape. For example, since 18 Gabor elements created the shape, at 50% spatial coherence, 9 of the 18 Gabor elements would be randomly selected to have a random, rather than colinear, orientation. This ”learning period” contains the trials analyzed in this study. Monkey Z underwent this coherence training protocol for 43 days, and Monkey J for 46 days. At the lowest coherence (50%), the task is extremely difficult (Figure 1c), which allowed for quantifiable improvements in performance over time. Performance at low coherences (50 and 62.5%) showed the most improvement (see Figure 3), and only these trials were utilized in learning analyses (with the exception of Figure 3a-b). Both animals performed near 100% for this highest coherence throughout this period, indicating that they were familiar with the nature of the task, and any increases in performance were stimulus, and not task, related.

2.2.3 Data Analysis

Pooling and Moving Average To verify that learning occurred, we first analyzed performance over 1000 trials of low coherence presentations at the beginning and end of the training period. To examine the dynamics of learning, we also computed moving averages over 300 trial windows, shifting 50 trials per successive window.

Learning Classical measures of learning included detection rate and reaction times. Detection rate was computed from correct trials divided by the sum of correct and fail trials. Reaction times were computed as the difference between saccade and shape onset. Both were computed as pooled (early/late), as well as a

moving average.

Electrophysiology LFPs were initially sampled at 10kHz and then downsampled to 1kHz. For all analyses, local field potentials (LFPs) were filtered from 2-100Hz using an 8^{th} order Butterworth filter. We chose a large filtering range to allow for visualization of broad amplitude changes in event aligned analyses, as well as more specific changes in mutual information (MI) analyses. A range of LFP frequencies have been implicated as related to spikes (Manning et al., 2009; Rasch et al., 2008), BOLD signals (Logothetis et al., 2001), and cognition (Rutishauser et al., 2010; Rey et al., 2015), and given the novelty of studying LFPs in relation to VPL, we wanted to allow for both broad- and narrow-band changes. However, given the short timescales of the stimulus associated decisions, signals below 2 Hz would not be of interest and, especially in one animal, largely reflected motion artifacts. After filtering, LFPs were then "cleaned", in order to handle noise issues that arose. We rejected periods with very average high or low amplitudes that occurred for 100ms or longer ($<$0.001 mV or $>$100000 mV) and blank periods where the mean signal was lost. We also rejected individual electrodes that were poorly correlated ($r<.7$) to the mean across all electrodes on a given day. We also rejected electrodes on a day by day basis if their mean amplitude was ($>$2000 mV) after this "cleaning" process. Finally, we also rejected undersampled electrodes (with fewer than 75 correct detections over the analyzed set of trials). These sampling criteria resulted in completely eliminating 4 out of 96 electrodes for Monkey Z and 8 out of 96 electrodes for Monkey J, with others only eliminated on a given day or moving average point. On a day by day basis, 1-3 ($<$4%) electrodes were eliminated for Monkey Z for most days. For Monkey J, $<$10% of 96 electrodes on average were eliminated per day on most days.

Statistics All r values are reported as Pearson's correlation, r^2 as the square of Pearson's correlation (with the exception of where a partial, Spearman's rank, correlation is indicated), linear fits from a simple linear regression, and all p values reported are from a paired t-test or comparison to a mean of zero, as indicated. Error bars and shaded regions are reported as standard error of the mean.

Event Aligned Analysis For event aligned analyses, processed LFPs were aligned to a given event, either

the shape appearance (sensory event) or the saccade (choice event), and averaged according to behavioral performance (correct or fail for stimulus aligned and correct or false alarm for saccade aligned). To look at decision-relevant signaling, we analyzed responses over a 75 ms window (125-200ms post-shape, 100-175ms pre-saccade) within the typical reaction time of detection.

Mutual Information Analysis We computed mutual information (MI) between events (stimulus, saccade, or neural response) to quantify the reduction in uncertainty about one task event, given knowledge of another task event (Ghose and Harrison, 2009; Harrison et al., 2013; Weiner and Ghose, 2014; Weiner and Ghose, 2015). Trials were parceled into bins to obtain event distributions on the particular time scale of the bin (Figure 2a). Mutual information (reliability), quantifying the ability of one event type to inform another, was then computed for this temporal resolution (binwidth) and by varying the temporal interval (delay) between the two types of events. For behavioral information, quantifying the relationship between shape presentation and saccades, delays varied from 25 to 500 ms (Figure 2b), and for sensory information, quantifying the relationship between shape presentation and neuronal response, and choice information, quantifying the relationship between neuronal response and saccades, delays from 25 to 250 ms were examined (Figure 2c). This process was then repeated by reparcelling the data for a variety of binwidths (from 25 to 250 ms). Thus, we computed mutual information from contingency tables constructed as a function of binwidth and delay (interval between bins). We also computed behavioral information, where the contingency table is 2x2 in size (shape/no-shape and saccade/no-saccade). Since behavioral information incorporates hit rates and false alarms, this moment to moment analysis is equivalent to a discriminability (d') measure, but without the underlying assumptions of normality inherent to the z-scoring done in a d' analysis. Additionally, a d' measure would not be directly comparable to sensory and choice reliability, whereas behavioral reliability is.

To form a similar contingency table for neuronal responses within bins, we adopted a similar approach as we have previously used to examine responses distributed across multiple electrodes. We used a variation of a Fisher linear discriminant analysis process, where LFPs were randomly divided into training and test sets

(50% of the data for each) (Figure 2c). From the training set, we separately computed the average LFP from event positive and event negative bins. We subtracted those two averages to form a LFP discriminant, taking into account the variance. The projection of every observation from the test set onto the discriminant was computed by dot product, and the resulting distribution of projections was then binned into 20 categories. Thus, the contingency tables for sensory and choice information, which were compiled separately for each electrode, were 2x20 in size. Mutual information was computed for each temporally specific contingency table (Figure 2d). To facilitate comparison across different binwidths, this is then converted to a mutual information rate (bits/s) by dividing by the binwidth, referred to in the results as "reliability". Sensory information, examining the relationship between the presence or absence of a shape and neuronal response, and choice information, examining the relationship between the occurrence of saccades and neuronal responses, were analyzed in an analogous manner.

Co-variance Correction When computing MI, we corrected for the co-variation between sensory and choice events based on behavior. Sensory and choice signals necessarily co-vary with behavioral performance. For example, if we were looking at a reflex, a purely sensory neuron's responses would be highly predictive of the subsequent motor act simply due to the high behavioral correlation between the sensory stimulus and motor act. Because there is not a 100% correlation between the stimulus and the act associated with choice in a challenging decision such as ours, this covariance issue is not as challenging as it would be for a reflex, but it still poses a challenge for trying to dissociate sensory and choice related signals. Fortunately, our contingency table approach offers a solution; we can use the statistics of the relationship between sensory stimuli (shapes) and motor choices (saccades), in the form of behavioral information, to predict the choice information that would be expected by chance given sensory information, and the sensory information that would be expected by chance given choice information. The "chance" level of information is then subtracted by the raw information to yield a behavioral covariance corrected measure (Ghose and Harrison, 2009). We also computed the analysis without the covariance correction. While the correction was neces-

sary to disassociate sensory and choice reliability, it could also create the correlations to behavior, since the relationship between the stimulus and saccade (behavior) is what is subtracted in the covariance correction. This did not appear to be the case, however. Statistical results and distributions were similar to those with the correction.

Peak Analysis Once information surfaces were computed across all binwidths and delays, we summarized all information surfaces according to the maximal information observed within a temporal window of interest (peak reliability) and averaged this peak across electrodes, time points, etc. In this way, peak reliability allowed us a single measure that could be correlated across various points in time or electrodes on the array, and direct comparisons to sensory, choice, behavior, and/or predicted behavior could be made, with correlations containing pooled measures that individually are corrected for covariance on a moment to moment basis. For physiological responses, the window, that peaks were extracted from, matched the time which, given sensory and motor delays, detection relevant signals were likely to be present (125 to 200ms for sensory and -75 to 150ms for choice), within a binwidth of 75-125ms. This window was also chosen for our event-locked average responses. To ensure peaks were unlikely to be due to chance, as MI contains an inherent positive bias (Treves and Panzeri, 1995), we also computed the information rate that would be expected by chance if there was no relationship between the stimulus and neuronal response. We resampled the contingency tables at each delay 100 times, which maintained the probability of observing any one variable but destroyed the relationship between stimulus and neuronal activity variables. We then set a cutoff value of 95% at a given delay, and if the original information value was not greater than this cutoff, it was set to zero. When the original value was greater (and thus considered significant), we subtracted the average resampled value to account for this bias.

As a final step to avoid falsely positive peaks, due to computing MI across many delays, we corrected for the expected false discovery rate that would be expected by chance (5% of the delays). We required that the number of delays with significant information exceed the expected number of false discoveries (0.05 times

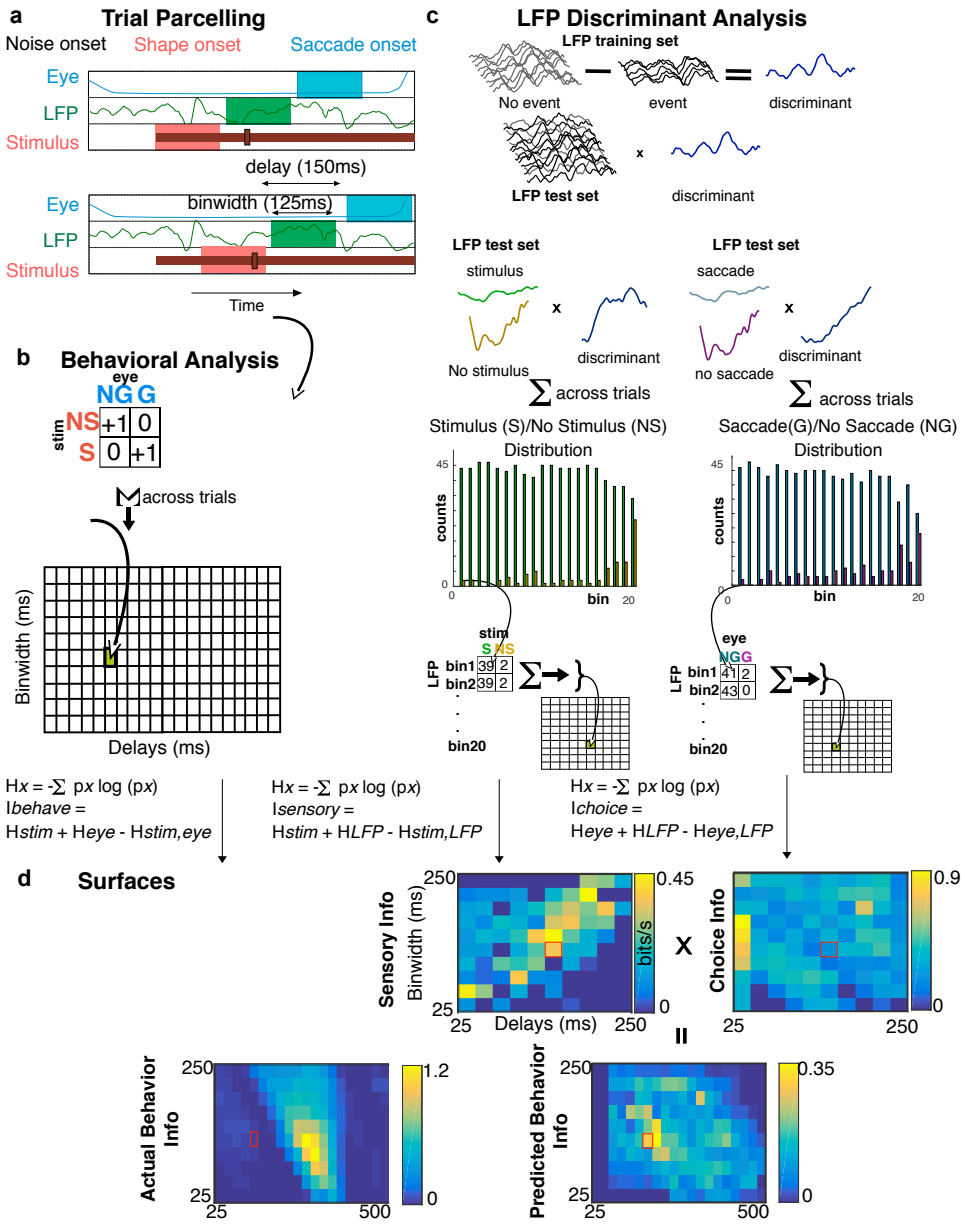

Figure 2: Mutual Information Method: a.) Neural signals and behavior were analyzed at varying binwidths and delays from the event, either the shape stimulus onset (sensory event) or the saccade (choice event). An example at 150ms delay and 125ms binwidth from example trials is used. b.) Behavioral information was calculated using a contingency table of the probability that the subject made a saccade/choice (G) or no choice (NG), given whether a shape was present (S) or not (NS). c) To construct a contingency table for LFPs, 50% of the LFP traces were separately averaged for events and non-events. The difference between these averages was used as a discriminant for the remaining traces, and the distributions of projections onto that discriminant were separately tabulated for events and non-events. These distributions were binned into 20 categories to compute MI. d.) Surfaces represent the output, where MI is divided by the binwidth to give reliability, for actual behavior, sensory, and choice surfaces. Sensory and choice surfaces are combined to create a predicted behavioral surface. Red boxes denote the output of the example.

the total number of delays). If this criteria was not met, the entire surface for a given event pair was set to zero reliability, and no peak was reported. This occurred for 6.7% and 7.0% of sensory and choice surfaces, respectively for Monkey J, and 2.6% for both sensory and choice surfaces for Monkey Z, across all moving average points and electrodes.

Predicted Behavior Additionally, we computed a predicted behavioral information surface by combining the sensory and choice surfaces. For every delay and binwidth, the predicted behavioral information describes the information rate that would result from the statistical relationship between sensory and choice information in a given population, if the behavior was completely informed by this population (Ghose and Harrison, 2009; Harrison et al., 2013; Weiner and Ghose, 2014; Weiner and Ghose, 2015). To do this, we computed the products of sensory and choice information for a given point on the predicted behavior surface by computing all possible sensory and choice delay combinations that could add to a given behavioral delay. We then found the maximum reliability within those possible sensory and choice delay combinations, and used this value for the prediction. For example, a behavioral delay of 200 could be found by a sensory delay of 100 and a choice delay of 100, or a sensory delay of 125 and a choice delay of 75, and so forth. We computed all possible combinations and then used the maximum value within those combinations. This predicted behavior surface could then be compared to the actual behavior, found through the behavioral MI process provided above, to establish how well a neural population could explain behavioral reliability, latency, and precision.

2.3 Results

2.3.1 Behavioral Performance

To study visual perceptual learning, we trained two monkeys over the course of several weeks to detect briefly presented shapes degraded by noise and report detection by a saccade to the shape. Both animals exhibited behavioral performance improvements in shape detection, i.e. learning, over the course of our observations. To demonstrate this, we analyzed behavior for both animals over the first and last 1000 trials

(referred to as early/late, respectively). Shape degradation was accomplished by decreasing the co-linearity of local oriented elements defining a specific shape. We define this as shape coherence which is 100% when the orientation of appropriately located elements was perfectly consistent with defining the shape, and 0% when the orientation of such elements was random. As expected in both animals and time periods, performance improved with shape coherence, with almost perfect performance at the highest coherence (Figure 3a). The dependence of performance on coherence clearly changes with training; while low coherence performance improves, high coherence performance does not improve for Monkey Z, and improves less than low coherences for Monkey J. This indicates that performance improvements during training at low coherences were not simply a result of increased task familiarity, but rather were specific to those stimuli that were particularly challenging. No substantial changes in reaction time for these low coherence stimuli were observed (Figure 3b), suggesting that changes in speed-accuracy trade-offs were not occurring during training. We selected the lowest two coherences (50% and 62.5%) for all further analyses for both animals, as the three highest and two highest coherences increased equally for Monkey J and Monkey Z, respectively, suggesting that improvements beyond the two lowest coherences were likely due to task, as opposed to perceptual, learning. For Monkey Z, early trials included 362 correct low coherence trials, 598 false alarms, and 209 false alarms; late trials included 456 correct low coherence trials, 653 false alarms, and 187 false alarms. For Monkey J, early trials included 187 correct low coherence trials, 441 false alarms, and 172 false alarms; late trials included 253 correct low coherence trials, 588 false alarms, and 35 false alarms. To examine the dynamics of perceptual improvements over the entire period of learning, and visualize any non-monotonic changes, we applied a moving average method to these low coherence trials by computing detection rates over consecutive blocks of 300 trials with 50 trial shifts. Consistent with the previous analysis, detection rate improved over time and between early and late periods (shaded regions) for both subjects. However, these improvements were not monotonic, but rather were characterized by up and down fluctuations in performance during the course of learning. Indeed, the correlation coefficient of detection rate vs trial, describing the fit of a linear

model of learning, was below 0.5 for both animals (Monkey J, r^2=0.38; Monkey Z, r^2=0.45) (Figure 3c).

2.3.2 Event Aligned Local Field Potentials

To look for neural population signals that might be responsible for detections during learning, we aligned the local field potentials (LFPs) across all electrodes (from a 96-electrode array implanted in V4) to both shape presentation and saccade initiation. If such signals play a role in the detection decisions made by the animals, we would expect an interaction between sensory and choice locked responses, such that, on average, sensory-aligned responses would differ depending on the eventual choice the animal made, and saccade-aligned responses would differ depending on the presence or absence of a shape.

Stimulus-Aligned: Sensory In accordance with this prediction, we found that for both early and late trials, the amplitude of the shape response was larger prior to correct detections, as opposed to false alarms, in both individual electrodes and over the sampled population of electrodes (Figure 4a), for both animals. For Monkey Z, this difference also increased in late trials. To examine whether particular electrodes carried strong detection relevant information, we mapped the RMS amplitude of sensory locked responses from correct trials over the time window in which differences were observed according to the stimulus (125-200 ms). Individual electrodes showed an increase in amplitude in late trials; this was significant for Monkey Z (paired t-test, $p<<.001$), but not Monkey J ($p=.10$). We also found that the spatial pattern of stimulus aligned responses across the array did not substantially change with learning; the electrodes with the strongest responses prior to learning maintained their relatively strong responses throughout training (Monkey Z: r=0.85, Monkey J: r=0.71). All correlations were highly significant ($p<<0.001$). Thus, in trial averages, training appeared to produce gain-like effects on the magnitude of perceived shape responses across the array (Figure 4c).

Saccade-Aligned: Choice We performed a similar event-locked analysis with respect to saccades, when the stimulus was present and perceived (correct) and when the stimulus was not present but still perceived (false alarm). Consistent with previous observations (Tolias et al., 2001), all electrodes displayed a strong pre-saccadic signal. Prior to that signal, and given typical reaction times, roughly corresponding with the

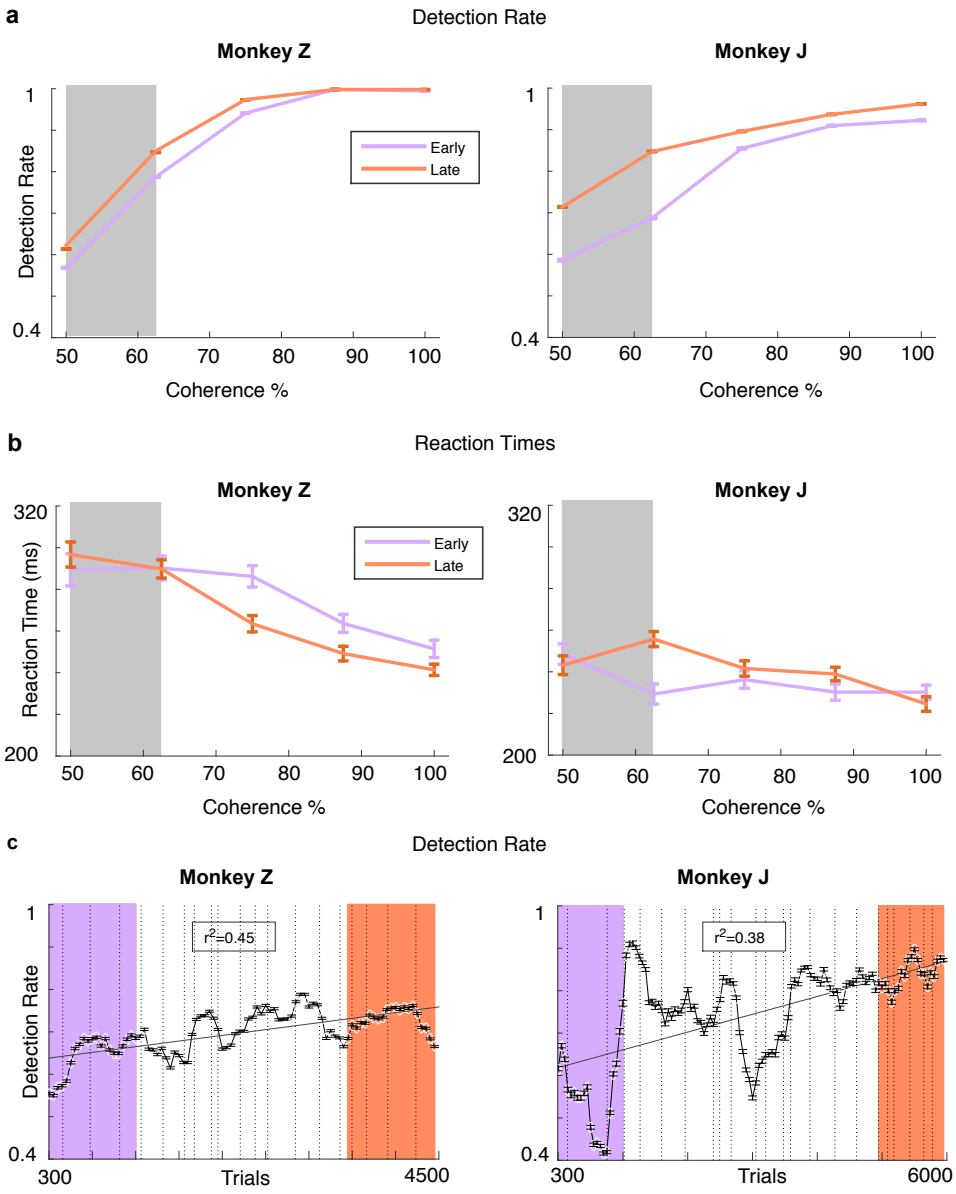

Figure 3: Performance Measures Over the Course of Perceptual Learning: a.) Detection rate (hits/hits+failures) increases with coherence and improves in late trials for both animals, particularly at low coherences (shaded region). b.) Reaction times decrease with higher coherences but do not change between early and late trials for low coherences. c.) There is an overall improvement as training progresses for both animals in detection rate. Learning is not monotonic; there are noticeable day to day fluctuations with learning for detection rate, especially for Monkey J, as indicated by the r^2 values for the linear fit of the line to the data (Monkey Z: detection, r^2=0.45; Monkey J: detection, r^2=0.38). Gray lines represent the linear fit and dotted lines represent individual days. Error bars represent SEM, of a binomial distribution where applicable.

same time window that revealed choice effects on shape responses, we observed shape effects on saccade-locked responses (-100 to -175ms). In early trials, there is no average difference between correct and false alarm trials for either animal. However, correct, but not false alarm, trials increase in amplitude for Monkey Z after learning. Monkey J, similarly to stimulus aligned LFPs, does not show an increase in the event aligned averages over time (Figure 4b) As with shape-locked responses, saccade locked responses for correct trials were also spatially heterogeneous and consistent with gain-like effects for both animals (Monkey Z: r=0.86; Monkey J: r=0.59), and there was a significant increase for both animals (Monkey Z: paired t-test, $p<<0.001$; Monkey J: p=0.01) (Figure 4c). All correlations were highly significant ($p<<0.001$). We also correlated sensory and choice RMS measures of each electrode for both early and late trials, to ask whether the same populations that were high for sensory (stimulus-aligned) effects were also high in predicting the choice (saccade-aligned). As expected, given that both analyses look at similar windows on correct detection trials, sensory and choice measures were highly correlated for both animals in both early and late trials (Figure 4d) (Monkey Z: early r=0.74, late r=0.95; Monkey J: early r=0.85, late r=0.92). All correlations were highly significant ($p<<0.001$).

2.3.3 Mutual Information

The observation that average LFP signals, within reaction time limited epochs, depend on both the presence of a shape and impending saccade execution, suggests such signals may play a role in perceptual detection (Shadlen and Newsome, 2001; Romo et al., 2004). Furthermore, our finding that these signals increased in magnitude over the course of training for almost all electrodes in Monkey Z, and many electrodes in Monkey J (Figure 4c), suggests that they may be contributing to learning. However, the presence of activity deviations within reaction time limited epochs on average does not mean that such activity occurs consistently on a trial to trial basis. For example, the broad peak of activity seen in the reaction time defined window of the shape-locked responses (Figure 4a) could reflect the superposition, across trials or electrodes, of narrow peaks of activity of variable latency. Similarly, the average amplitude might reflect the rare occurrence of

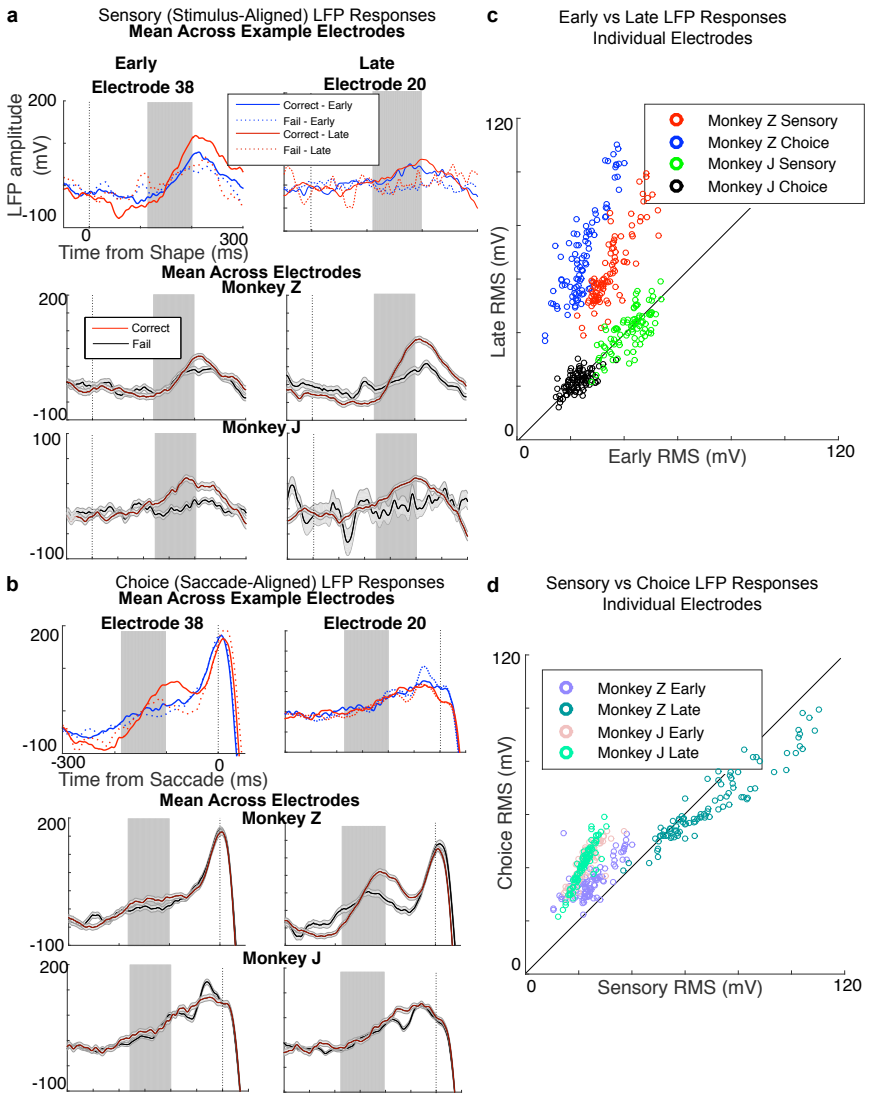

Figure 4: Trial Averaged Event Aligned LFPs: a.) Both subjects show enhanced stimulus aligned LFP effects (stimulus at dotted line at 0ms) on correct trials compared to failure trials before and after learning in examples and averages. b.) Monkey Z shows enhanced saccade aligned LFP effects on correct trials compared to false alarm trials in examples and averages after learning (saccade at dotted line at 0ms). Shaded SEM is the width of aligned traces. c) When the root mean squared (RMS) of the LFP amplitude (shaded area a:25 to 200ms, b:-100 to -175ms) was found for each electrode and averaged across correct trials, both animals shows gain-like effects in correct shape and saccade aligned LFP responses between early and late phases of training, but only Monkey Z showed amplitude changes between the early and late trials for stimulus aligned (Stimulus Aligned: Monkey Z: r=0.85, paired t-test, $p<<0.001$; Monkey J: r=0.71, p=.10), while both increased in late trials for saccade aligned (Saccade Aligned: Monkey Z: r=0.86, paired t-test, $p<<.001$; Monkey J: r=0.59, p=0.01). All correlations were highly significant ($p<<0.001$). d.) When sensory (stimulus aligned) and choice (saccade aligned) RMS values from correct trials for both animals were compared, they were also highly correlated, especially after learning (Monkey Z: early r=0.74, late r=0.95; Monkey J: early r=0.85, late r=0.92). Again, all correlations were highly significant ($p<<0.001$). Filled in scatter plot points correspond to example electrodes. Error bars represent SEM. 88/96 and 92/96 electrodes were used for Monkey J and Monkey Z, respectively.

strong activation rather than any consistent signal. Additionally, averages may obscure changes over learning that occur over the moment to moment timescale demanded by the task. For example, a purely trial-based analysis ignores the large periods of correct rejection in trials for which shapes were only presented after many seconds of fixation. A final concern, which is particularly relevant for localizing where in the visual pathway learning related changes may be occurring, is the temporal overlap between shape-evoked and pre-saccadic activity (Figure 4a-b). This makes it hard to infer whether potential LFP changes observed during perceptual learning reflect changes in the feedfoward shape-related signals, feedback saccade-related signals, or some combination of the two.

Reliability Changes with Learning To measure the consistency of moment to moment variations in LFP across individual trials, we utilized an analysis that employed information theory to compute the mutual information (MI) between LFPs, shapes, and saccades at a range of binwidths (25-250 ms) and delays (25-250 ms). MI measures how reliably one can infer the state of one event given another event, and notably incorporates the uncertainty of both events. We convert this into a rate by dividing the mutual information for a given delay and binwidth by that binwidth, to get a rate of bits/s, which we refer to as ”reliability”, since it measures how reliably LFPs reflect shape appearance (sensory) or predict the saccade (choice). Thus, by computing MI at fine timescales, we can answer the question of how reliable signals are on a moment to moment basis.

We apply the same analysis to measure how reliably saccades reflect shape appearance (behavior). Importantly, this behavioral information allows us to correct for the expected covariance of sensory and choice (see Methods), disassociating sensory and choice information. All of these MI rates (reliability) were compiled into a surface describing how the moment-to-moment correlations between two variables depend on timing parameters. A final advantage of this technique is the ability to use sensory and choice information surfaces to generate, without any modeling, a predicted behavioral information surface that describes what behavior would be expected if the measured signal alone was responsible for detection decisions.

Sensory and choice surfaces based on the LFPs from single electrodes showed increases in peak reliability after learning (Figure 5a-b) over the window of temporal parameters used in the previous RMS analysis (white box). To evaluate the potential contribution of individual electrodes to this performance improvement, we generated behavioral prediction surfaces on the basis on sensory and choice information surfaces. Such a surface describes what behavioral information would be expected if the electrode were the only signal responsible for decisions. By performing this analysis before and after learning, we were therefore able to quantitatively measure the potential behavioral impact of physiological changes occurring at single electrodes. All electrodes examined showed dramatic increases in predicted behavioral reliability consistent with those actually observed, and without accompanying changes in behavioral timing (Figure 5c).

Peak Reliability Distribution The location of peak reliability, at both delays and binwidths, on average, was consistent across learning, and only changed by $<$6ms for all measures (sensory, choice, and predictions), for both animals, indicating a stability in temporal parameters after learning. In contrast to these temporal parameters, peak height, or peak reliability, reflecting the reliability of detection, increased dramatically with training in both animals (Figure 6). These findings are consistent with classical measures of performance (Figure 3), and document that shape learning in this task was characterized by increases in performance, but not changes in timing.

To assess spatial organization of task relevant information across the array, we analyzed the autocorrelation of peak reliability across the array. Sensory and choice peak reliability, on average, for Monkey J, had correlations of r=0.07, r=-0.03, r=0.09, and r=-0.02 for early and late sensory and early and late choice, respectively, between neighboring (400 μm distant) electrodes. For Monkey Z, the average correlation had values of r=0.23, r=0.06, r=0.20, and r=0.20 for early and late sensory and early and late choice, respectively, between neighboring electrodes. This is in contrast to RMS autocorrelations, which were much higher (Monkey Z: r=0.79, r=0.72, r=0.74, r=0.71; Monkey J: r=0.22, r=0.13, r=0.25, r=0.13, for early and late sensory and early and late choice, respectively). We also correlated the RMS and peak reliability of individual

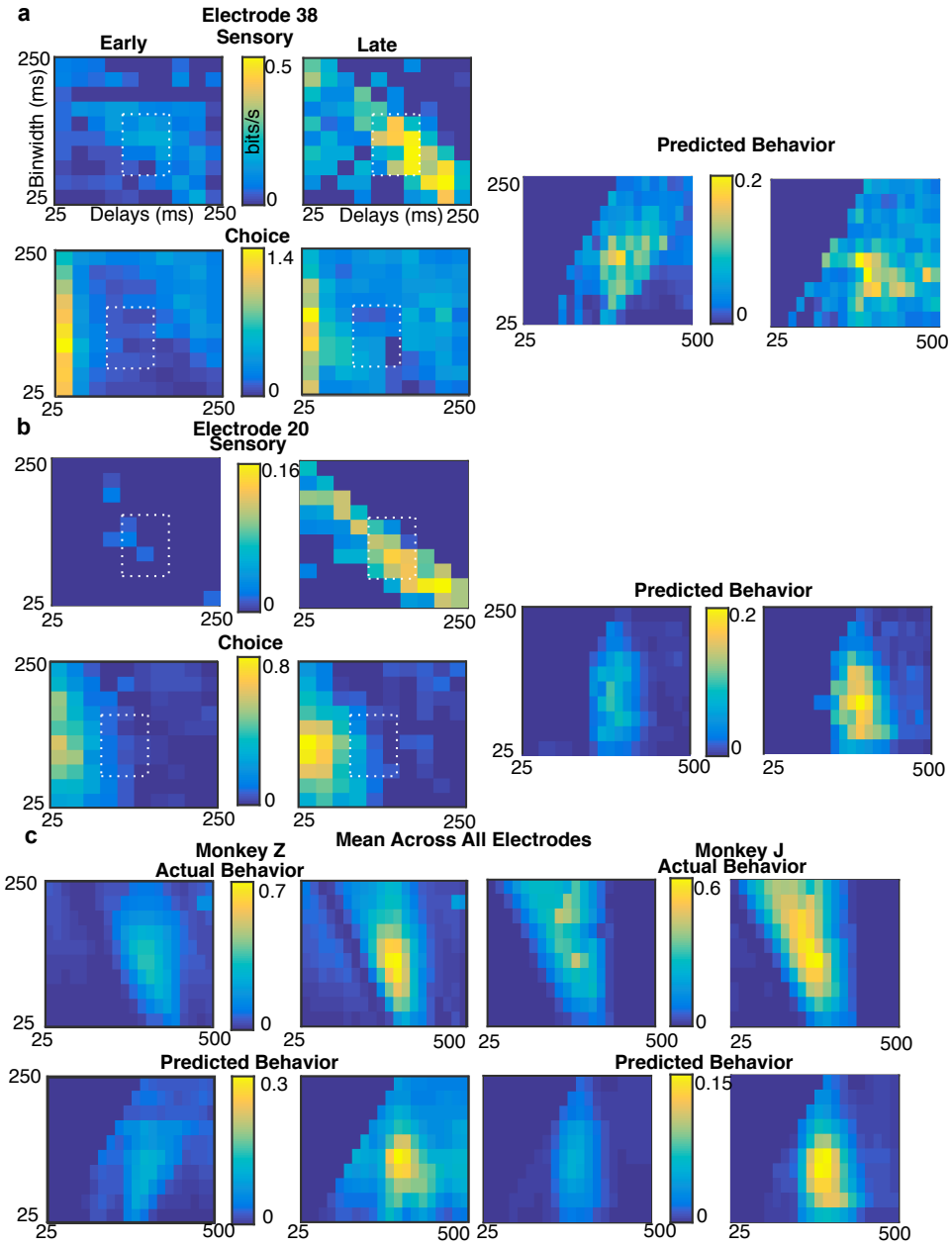

Figure 5: Mutual Information Surfaces: a-b.) Example electrodes show an enhancement, especially in sensory, but also in choice, reliability in late trials compared to early. Combining sensory and choice surfaces into a behavioral prediction surface shows that individual electrodes can largely predict behavioral reliability and timing. White boxes indicate the delays (125-200 ms for sensory, -100 to -175 ms for choice) and binwidths (75-125 ms) inferred from the event-triggered analyses as potentially decision relevant. c.) Both animals show improvements after learning when reliability between eye movement and stimulus presence (behavioral information) is analyzed for early and late trials, within a reasonable reaction time (delay) from the stimulus. Predicted behavior, computed by combining the sensory and choice surfaces (see Methods), accounted for about $1/3$ of the actual behavior when averaged across electrodes and had similar temporal dynamics in its peak reliability. 88/96 and 92/96 electrodes were used for Monkey J and Monkey Z, respectively.

electrodes, to assess how similar the summarized results of these measures were. For Monkey J, early and late sensory and choice RMS measures were well correlated with peak information, but less so for Monkey Z (Monkey J: early sensory r=0.54, late sensory r=0.44, early choice r=0.62, late choice r=0.37; Monkey Z: early sensory r=0.59, late sensory r=0.20, early choice r=0.39, late choice r=0.19). Thus, such correlations decreased in all measures after learning. This suggests that RMS measures may be susceptible to spatial correlations in activity that occur on behaviorally irrelevant timescales, especially after learning.

Despite the increased independence of electrode sampling in the MI analysis, for almost all electrodes, we see large improvements in the amplitude of sensory, choice, and predicted behavioral reliability associated with learning ($p<0.001$ for all measures and both animals), in conjunction with improvement in actual behavior (Figure 6d). In contrast to RMS measures (Figure 4), reliability heterogeneity was not consistent between early and late periods (Monkey Z: sensory r=0.04, choice r=0.18, predicted r=0.64; Monkey J: sensory r=0.17, choice r=0.14, predicted r=0.35, all correlations were highly significant $p<<0.001$ except Monkey J sensory was significant at p=0.01) (Figure 6a-c). However, many reliability measures increased by a similar late:early ratio. (Monkey Z: sensory= 2.18, choice=2.50, predicted=1.83, actual=1.18; Monkey J: sensory=1.97, choice=1.33, predicted=2.07, actual=1.07)

Previous analyses of single unit and neuronal ensemble data with this task revealed a strong correlation between sensory and choice reliability (Weiner and Ghose, 2014; Weiner and Ghose, 2015), such that reliable choice information was only observed for neurons that carried reliable sensory information. To examine whether this relationship also applied to LFPs, and was subject to change with learning, we correlated sensory and choice for each electrode separately for the early and late periods of training. Sensory and choice reliabilities were consistent within an electrode, despite the covariance correction contained in our MI analysis. There were also high correlations between sensory and choice peak reliability, for both animals, in both early and late trials, with the exception of Monkey Z in the early period (Monkey Z: early, r=-0.16, late, r=0.53; Monkey J: early, r=0.69, late, r=0.49, all correlations were highly significant $p<<0.001$) (Figure 6e).

Consistent with more precise methods, we found that the populations highest in sensory reliability were also high in choice reliability, and both were strongly correlated after learning. This suggests that the most reliable neurons were playing the strongest role in decision making after learning. It is less conclusive, however, about whether this is associated with learning improvements or required for learning, given that Monkey Z, but not Monkey J, had low correlations before learning.

Peak Reliability Dynamics To ask whether LFP reliability fluctuates over the course of learning (Figure 7a-b), we computed sensory, choice, and predicted behavior information peaks using the same moving average sampling as was done previously for detection rate (Figure 3). As with the classic behavioral metrics, we found that reliability increases were non-monotonic over the course of learning. To understand whether such fluctuations in LFP reliability were related to performance, we also computed peak behavioral reliability over the entire course of learning within non-overlapping blocks of 300 trials (in order to avoid spurious correlations that could occur with overlapping blocks). We used a Spearman's partial correlation to control for the interaction between sensory and choice. We found that sensory peak reliability, and the predicted behavior peak reliability, covaries with actual behavior peak reliability, while choice does not, across examples (Figure 7a), the mean (across all electrodes: Monkey Z: r=0.67, r=0.07, r=0.67; Monkey J: r=0.60, r=-0.27, r=0.33, respectively) (Figure 7b), and individual electrodes (Figure 7c). This suggests that sensory interactions were driving the correlations to behavioral fluctuations, and that changes in choice signals were driven by their relationship to the sensory signals. We also correlated the predicted and actual behavior and found that 64 electrodes had significant correlations in Monkey Z and 14 in Monkey J. (Figure 7d).

Spatial Independence and Redundancy We also assessed whether peak reliability of a given electrode depended on the peak reliability of nearby electrodes. While autocorrelations of reliability were low across the array, as were correlations between early and late trials, it could be that reliability is distributed in a heterogeneous manner but still spatially dependent, with redundancy depending on distance across the array. We assessed this for a subset of neighboring electrodes for Monkey Z (28 pairs), by comparing the sum of

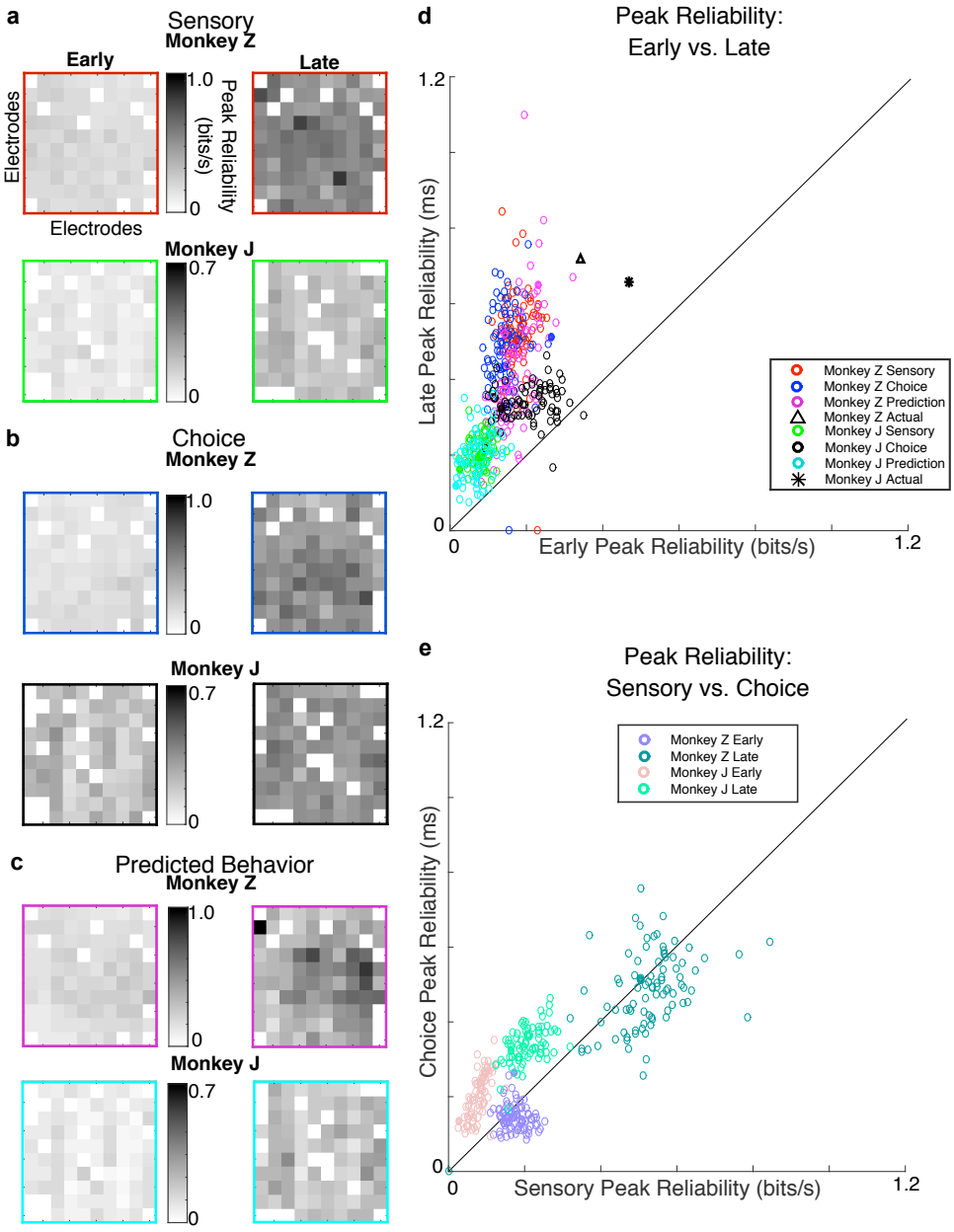

Figure 6: Peak Reliability: a.) Sensory, b.) choice, and c.) predicted peak reliability across the array was heterogeneous but, unlike RMS measures, not consistent between early and late phases (Early/late correlations: Monkey Z: sensory r=0.04, choice r=0.18, predicted r=0.64; Monkey J: sensory r=0.17, choice r=0.14, predicted r=0.35, all correlations were highly significant $p<<0.001$ except Monkey J sensory was significant at p=0.01) d.) There was a significant effect of learning for both animals for both sensory and choice populations (paired t-test, $p<<0.001$). Almost all electrodes showed an improvement in peak reliability after learning, for both animals. Sensory, choice, predicted behavior, and actual behavior increased by similar late:early ratios. (Monkey Z: sensory= 2.18, choice=2.50, predicted=1.83, actual=1.18; Monkey J: sensory=1.97, choice=1.33, predicted=2.07, actual=1.07) e.) Sensory and choice peak reliability were well correlated, except in early trials for Monkey Z. (Monkey Z: early, r=-0.16, late, r=0.53, Monkey J: early, r=0.69, late, r=0.49, all correlations were highly significant $p<<0.001$) Filled in scatter plot points correspond to example electrodes. 88/96 and 92/96 electrodes were used for Monkey J and Monkey Z, respectively.

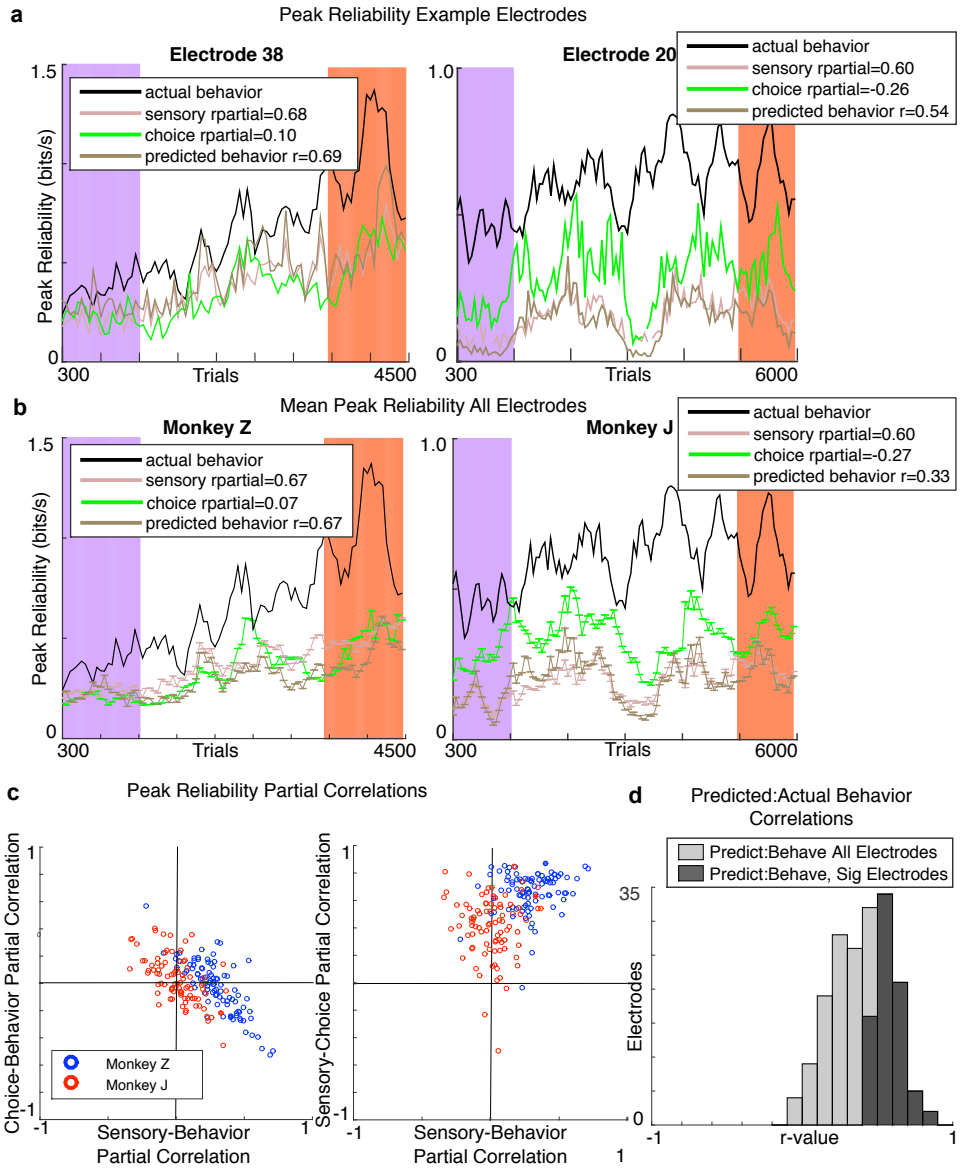

Figure 7: Peak Reliability and Behavior: a.) Example electrodes had sensory and predicted behavior timecourses of peak reliability which followed behavior well, while choice peak reliability does not. b.) The mean sensory and predicted reliability also followed actual behavioral fluctuations, while this was not the case for choice. (Monkey Z: sensory r=0.67, choice r=0.07, predicted r=0.67; Monkey J: sensory r=0.60, choice r=-0.27, predicted r=0.33) c.) Across all electrodes, sensory-choice correlations and sensory-behavior correlations, but not choice-behavior correlations, were significantly different from zero (t-test, $p<<0.001$). d.) Predicted timecourses were well correlated to actual behavior, with 64/92 electrodes being significant for Monkey Z, and 14/88 for Monkey J. Filled in scatter plot points correspond to example electrodes. Error bars represent SEM. Shaded areas represent early and late trials. 88/96 and 92/96 electrodes were used for Monkey J and Monkey Z.

peak reliability of neighboring electrodes to the peak reliability of those two electrodes when the LFPs from each electrode were concatenated prior to computation of MI. If the sum creates a stronger peak reliability than the concatenation, then there is spatial dependence, if this decreases as a function of distance. If this occurs but without a change over distance, then redundancy may be high but consistent across the array. Conversely, if there is no improvement in reliability, this suggests electrodes are entirely independent. It is also possible that concatenation could improve reliability in comparison to the sum, and this would suggest a synergistic effect.

We did find high levels of redundancy to be the case for immediate neighboring electrodes (Figure 8a). Reliability was higher for the summed pair vs the concatenated pair, at a high level of significance ($p<<0.001$). Concatenated reliability and summed reliability were correlated in some cases but not others (sensory: early r=0.66, late r=0.33; choice: early r=-0.03, late r=0.47). We then asked how this changes as a function of distance, looking at the peak reliability of a given electrode combined with an electrode two or three spaces away (rather than one away, as with the immediate neighbor electrodes). We found that electrode sums of pairs of up to three neighbors away were still more reliable then the concatenated pairs, suggesting that there may be a high level of redundancy across the array. For +2 electrodes, the increase was significant ($p<<0.001$) for sensory and choice, although correlations again varied (sensory: early r=0.39, late r=0.16; choice: early r=0.02, late r=0.22). For +3 electrodes, again, all increased with high significance ($p<<0.001$), while correlations varied (sensory: early r=0.65, late r=0.11; choice: early r=0.03, late r=0.45). However, analyzing longer distances might reveal a distance at which electrodes become less redundant (improved by their sum compared to independent concatenation), revealing spatial dependency. These patterns were also true in example surfaces (Figure 9), where the sum consistently was more reliable than the individual electrodes and the concatenation of the two electrodes (while the concatenation and individual surfaces were generally similar), and this was consistently the case for a distance of up to three electrodes away.

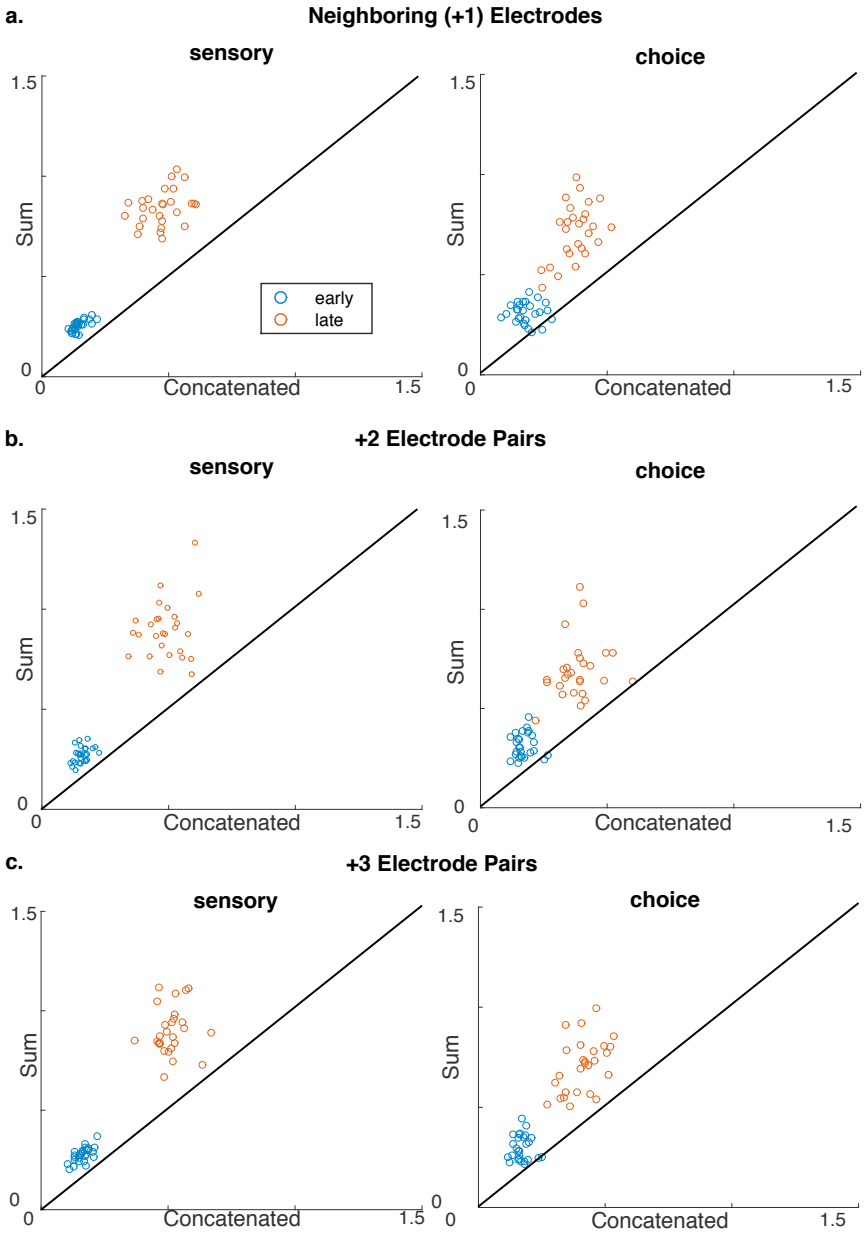

Figure 8: Peak Reliability of Individual, Concatenated, and Summed Electrode Pairs: a.) For neighboring electrode pairs, the peak reliability is far higher for the sum than the concatenation of the pairs for both early and late ($p<<0.001$) and is correlated for all except early choice (sensory: early r=0.66, late r=0.33; choice: early r=-0.03, late r=0.47). b.) For electrode pairs 2 electrodes away, the peak reliability is higher for the sum than the concatenation of the pairs for both early and late ($p<<0.001$) and is correlated for early sensory and late choice (sensory: early r=0.39, late r=0.16; choice: early r=0.02, late r=0.22) c.) For electrode pairs separated by a distance of 3 electrodes, the peak reliability is far higher for the sum than the concatenation of the pairs for both early and late ($p<<0.001$) and correlation was again high for early sensory and late choice, but not late sensory or early choice (sensory: early r=0.65, late r=0.11; choice: early r=0.03, late r=0.45). Electrodes are a subset of electrodes (28) from Monkey Z.

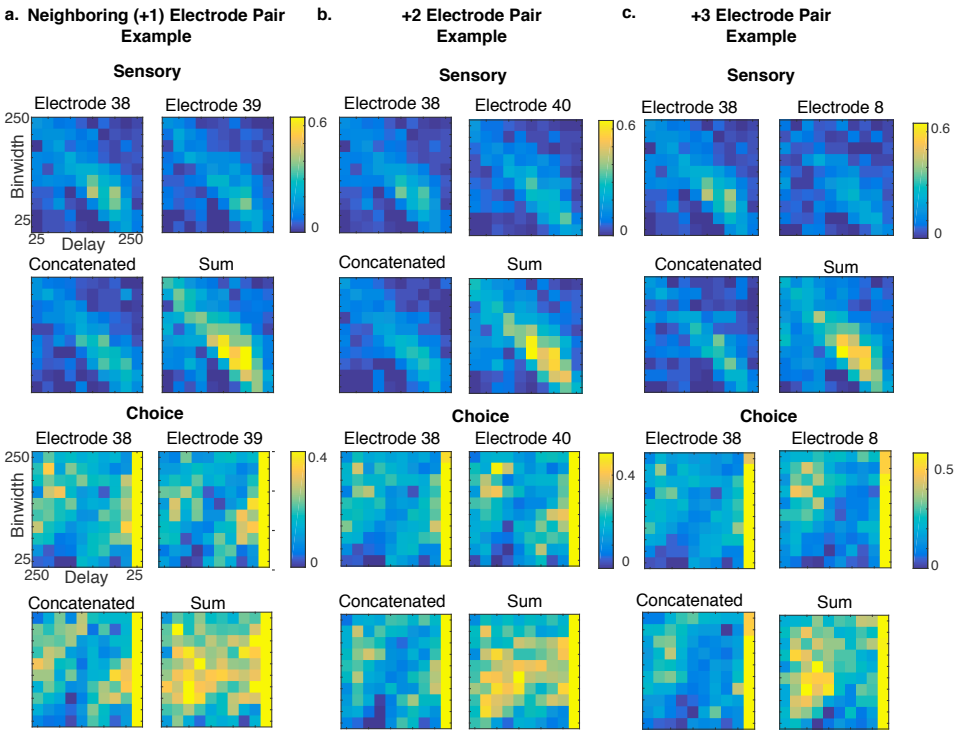

Figure 9: Electrode Pair Example Surfaces: a.) Sensory and choice surfaces for electrode pair 38 and 39, which neighbored each other (+1 electrode away). The concatenated surface appears similar to the individual electrode, but the sum shows increased reliability. This is the case for both sensory and choice. b.) Sensory and choice surfaces for electrode pair 38 and 40, where electrode 40 is 2 electrodes distant from electrode 38. Again, the summed surface is similar in reliability and temporal dynamics to the individual surfaces, but the summed surface demonstrates increased reliability. c.) Sensory and choice surfaces for electrode pair 38 and 8, where electrode 8 is three electrodes away. Results are similar to a.) and b.). Thus, redundancy across the array is high, at least in Monkey Z to up to a distance of 3 electrodes away.

3 Experiment 2: Individual Voxels are modulated by attention but not choice in area V4

3.1 Introduction

Due to previous work in our laboratory finding that feature based attention is targeted to specific, task appropriate neural populations in early visual cortex (Warren et al., 2014), we asked whether attention is similarly distributed in a task specific way in V4, how this depends on attentional state, and whether such neurons also signal the readout of the perceptual choice, given that choice signals have consistently been found in this area (see section on V4 in introduction). We designed a demanding stimulus discrimination task where we directed subjects to attend to a specific feature of the task during high-field fMRI scanning. The stimulus alternated continuously at varying frequencies in low and high level features (spatial frequency and shape, due to their expected sensory activation of V1 and V4, respectively). Voxels were measured at high resolution, sampling 1mm of cortex, from V1 to V4, and the stimulus was presented near perceptual threshold in order to disassociate the stimulus from the choice. We then used a linear regression analysis to compare continuous BOLD modulation of individual voxels to regressors modeling the continuous stimulus presentation when a given feature was attended to vs when it was not, and assessed how sensory and attention modulations overlapped with modulations containing a relationship to the ongoing perceptual choice. We found clear sensory attention effects in V4 that were specific to certain populations; however this did not appear to depend on initial sensitivity, and we did not see reliable choice signals or choice signals that overlapped with attention signals. We believe this may be due to the experimental design and recommend future approaches to disassociate sensory, attention, and choice signals in visual cortex.

3.2 Materials and Methods

3.2.1 Subjects and Data Acquisition

All procedures conformed to guidelines approved by the Institutional Review Board at the University of Minnesota. Four adult human subjects (two male, two female, one was the author of this manuscript and one was a PI on the author's committee) underwent functional magnetic resonance imaging (fMRI) in a 7 Tesla (7T) Siemens Magnetom scanner at the Center for Magnetic Resonance Research (CMRR) at the University of Minnesota with informed consent. All participants had normal or corrected to normal vision. Functional data were acquired using a T2*-weighted gradient-echo EPI sequence (45 slices, 1.6 mm x 1.6 mm x 1.6 mm, TR 900 ms, TE 22.8 ms, flip angle 50 degrees, multiband slice acceleration factor 3, partial Fourier 7/8, in-plane parallel factor 2). Fieldmaps were acquired with the same slice slab as the functional data for post-hoc correction of EPI spatial distortion (TR 566 ms, TE 4.69 ms and 5.71 ms).

3.2.2 Task and Training

The stimulus, created using custom code (http://www.ghoselab.cmrr.umn.edu/software.html), was composed of 20 Gabor elements (5 per quadrant, 4 degrees in size). Subjects viewed this stimulus using a mirror attached to the RF coil. A fixation dot was placed in the middle of the screen, and participants were instructed to fixate on the dot. The stimulus changed in three dimensions at separate, non-resonant frequencies: fixation dot color (pink or blue), shape (circle or diamond), and Gabor spatial frequency (high/thin or low/thick). The changes were not binary and occurred near the subject's perceptual threshold in the difficult/hard task; for example a shape could be nearly a diamond or a circle. The task consisted of six runs, with each run containing one easy and three hard trials that were 90 seconds long each, separated by 10 seconds of no stimulus. Participants were instructed to fixate on the dot at all times and to pay attention to one of the three changing features (dot color, spatial frequency, or shape), and continuously press a button on a button box when they perceived the circle, thin spatial frequency, or pink dot, depending on the run, and to release the

lever when they perceived the opposite extreme. In this way, we could disassociate the sensory stimulus from the choice/perception when the task was very difficult and near threshold. The fixation dot was used as a control; we expected to see very little sensory effects with this stimulus. Spatial frequency was used to compare a stimulus expected to activate earlier areas compared to shape. This generated four independent time series that could then be correlated to each other (Figure 10b): the time series of each of the three features, with one being attended per run, and the time series of the lever presses. The difficulty of the hard task was titrated based on a pre-test of the subject's performance; we aimed to have performance above chance, but not perfect, in order to disassociate sensory and choice signals.

3.2.3 Data Analysis

After standard motion correction and T1 alignment using custom MATLAB software, each time series from individual voxels was convolved with a canonical hemodynamic response function (HRF). The convolved time series was mean centered, in order to control for signal drift during the run, and then concatenated across runs and trials for each attention variable and task difficulty. Time series were then converted into percent BOLD (((signal-mean)/mean per trial) * 100) and z-scored. The signal was then regressed with 4 different regressors (sensory features and choice for the attended feature) to obtain beta weights which measured how well the BOLD signal was explained by the 4 regressors in the model below. Individual voxels could then be correlated and regressed based on their beta weights for various features, attention, and choice, or mapped across the visual system based on a given condition for a given region of interest (ROI). When subjects were collapsed, we aligned all subjects on an averaged atlas, created from the anatomical scans of all 4 subjects. Analyses for individual subjects were only aligned to their own T1 anatomical image. ROIs were defined using a Kastner atlas (Wang et al., 2015). We focus on shape responses, mostly in area V4 (referred to as hV4 in the Kastner atlas) for the purpose of this manuscript.

$$\mathrm{BOLD}_{\text{attended feature}} =$$

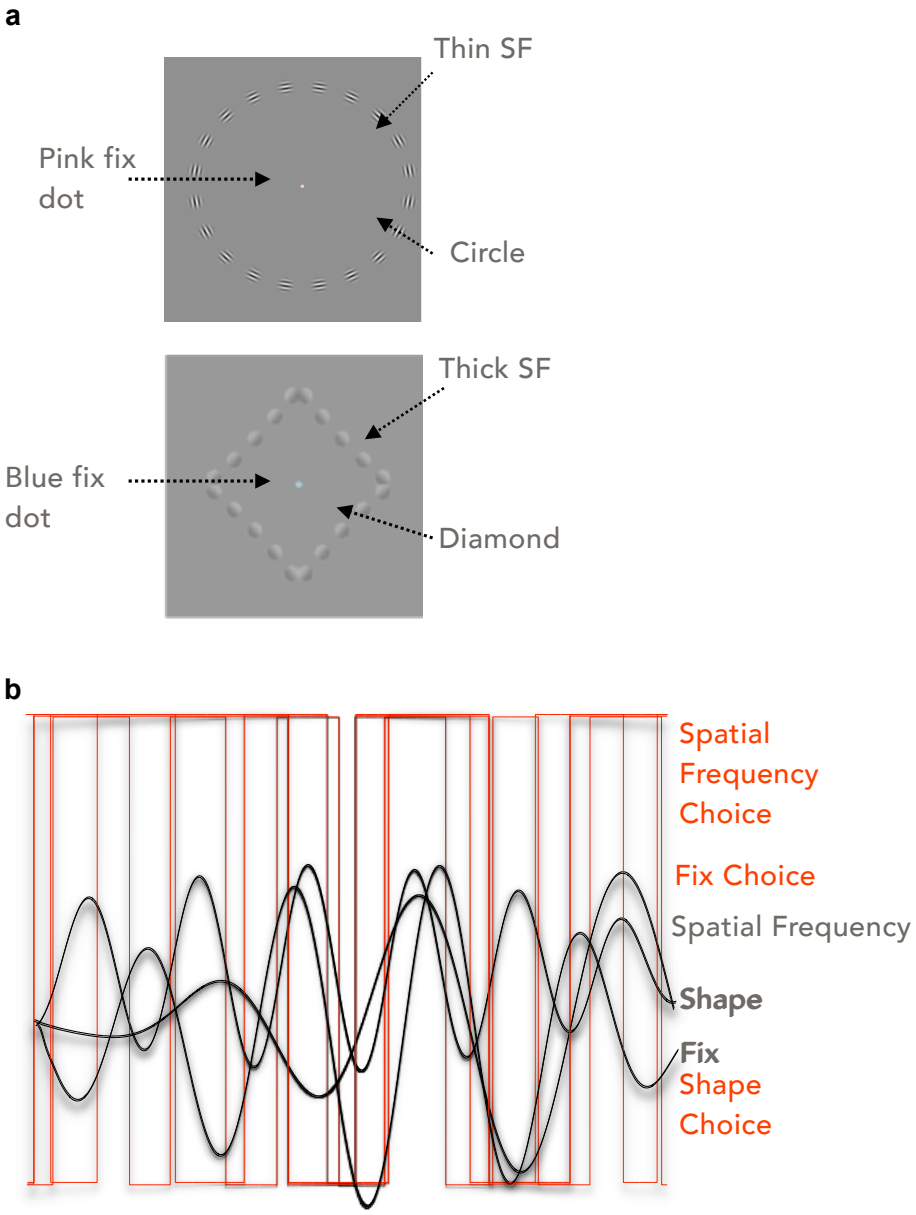

Figure 10: Attention Task: a.) The stimulus could vary in three dimensions; as a function of spatial frequency (SF), shape, or fixation color. These varied in a continuous manner at non-harmonic frequencies. Simultaneously, the subject made a binary choice, via a lever press, regarding the state of the stimulus (thin/thick spatial frequency, circle/diamond, pink/blue fixation dot) b.) Example timecourses of stimulus extremes for each feature and corresponding perceptual choices for the attend runs to each feature, which were used in the model to be regressed against the BOLD signal.

$$\beta_{\text{easy,SF}} * \text{SF}_{\text{hard}} + \beta_{\text{easy,Shape}} * \text{Shape}_{\text{hard}} + \beta_{\text{easy,fix}} * \text{Fix}_{\text{hard}} + \beta_{\text{Choice,hard}} * \text{Choice}_{\text{hard,attended feature}}$$

3.3 Results

3.3.1 Performance

To measure performance, we correlated (Pearson's correlation coefficient) the frequency of the attended stimulus to the frequency of the perceptual report. Subjects performed fairly consistently across almost all runs for all tasks in the hard trials. Performance did not saturate during the hard trials, creating a difference in the time course of the attended stimulus and the perceptual report. For hard attend shape trials, performance varied between r=0.55 and r=0.72 for all subjects, with an SEM between 0.01 and 0.03 across the 6 trials. For hard attend spatial frequency trials, performance varied between r=0.42 and r=0.70 (SEM between 0.02 and 0.03), and for hard attend fixation trials, performance varied between r=0.47 and r=0.85 (SEM between $<$0.01 and 0.04).

3.3.2 Sensory and Attentional Effects

We compared sensory beta weights for each voxel in areas V1v, V1d, and V4, across attend and no attend conditions. First, we collapsed all the subjects and measured the least square line fit of the two dimensional distribution (referred to as a line fit in the rest of the manuscript). V1 and V4 showed strong sensory effects for shape; however V4 also demonstrated attentional effects that V1 did not, as seen in Figure 12a, where the line fit is larger than 1 for V4 (1.3) but not V1d (1.0) or V1d (1.1). However, this effect was only clear on easy trials. We did not see strong sensory or attentional effects on hard trials when subjects were collapsed (Figure 12b). We then focused on V4, given attentional signals observed in easy trials. Spatial frequency and fixation sensory and attention signals were not as consistent in V1 or V4, and so we do not discuss those here.

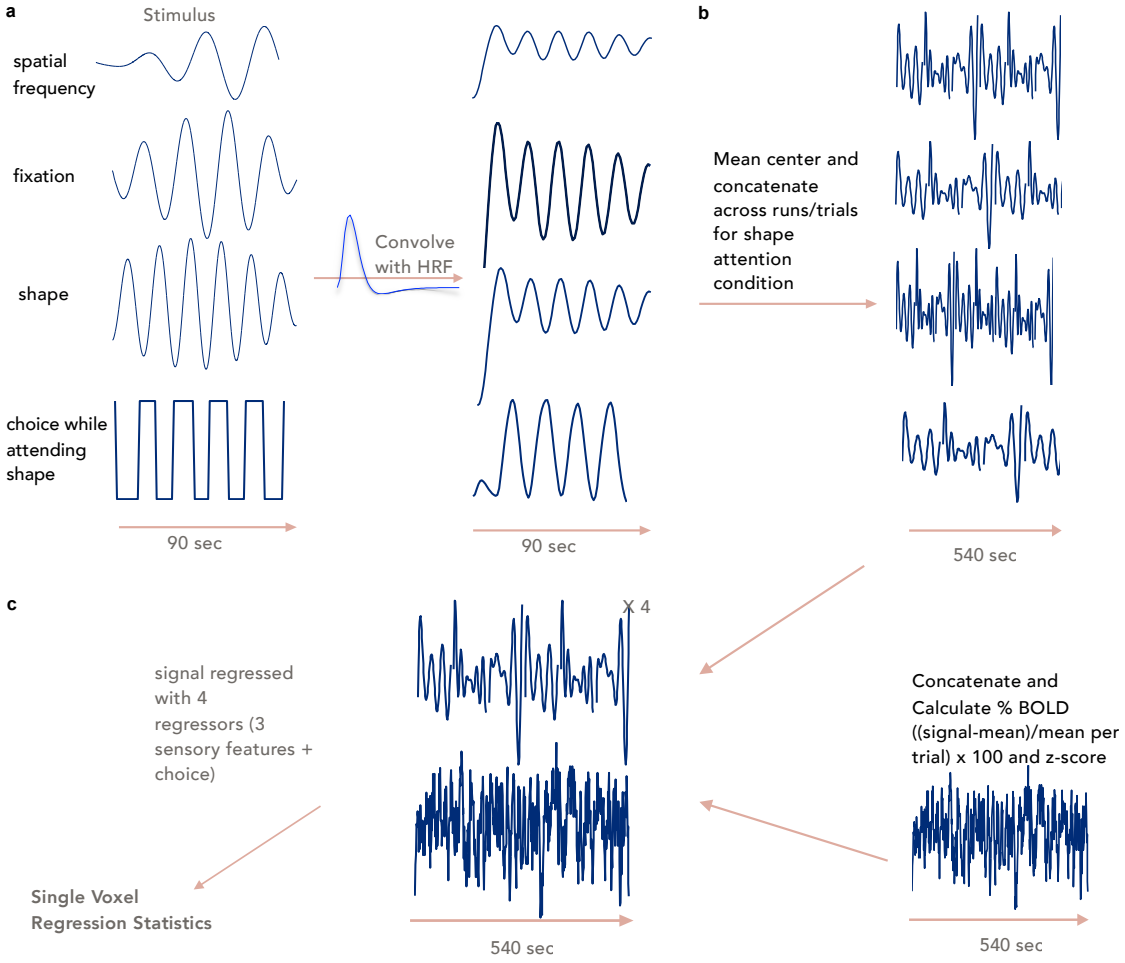

Figure 11: Individual Voxel Analysis: a.) Each stimulus, for a given feature (spatial frequency, fixation, or shape), and choice timecourses were convolved with a canonical HRF. b.) Timecourses were then mean-centered and concatenated across runs/trials for a given attention condition. c.) BOLD signals were similarly concatenated and converted to percent BOLD and also z-scored. d.) Feature/choice time courses were regressed against the BOLD signal to output four beta weights and an entire model fit.

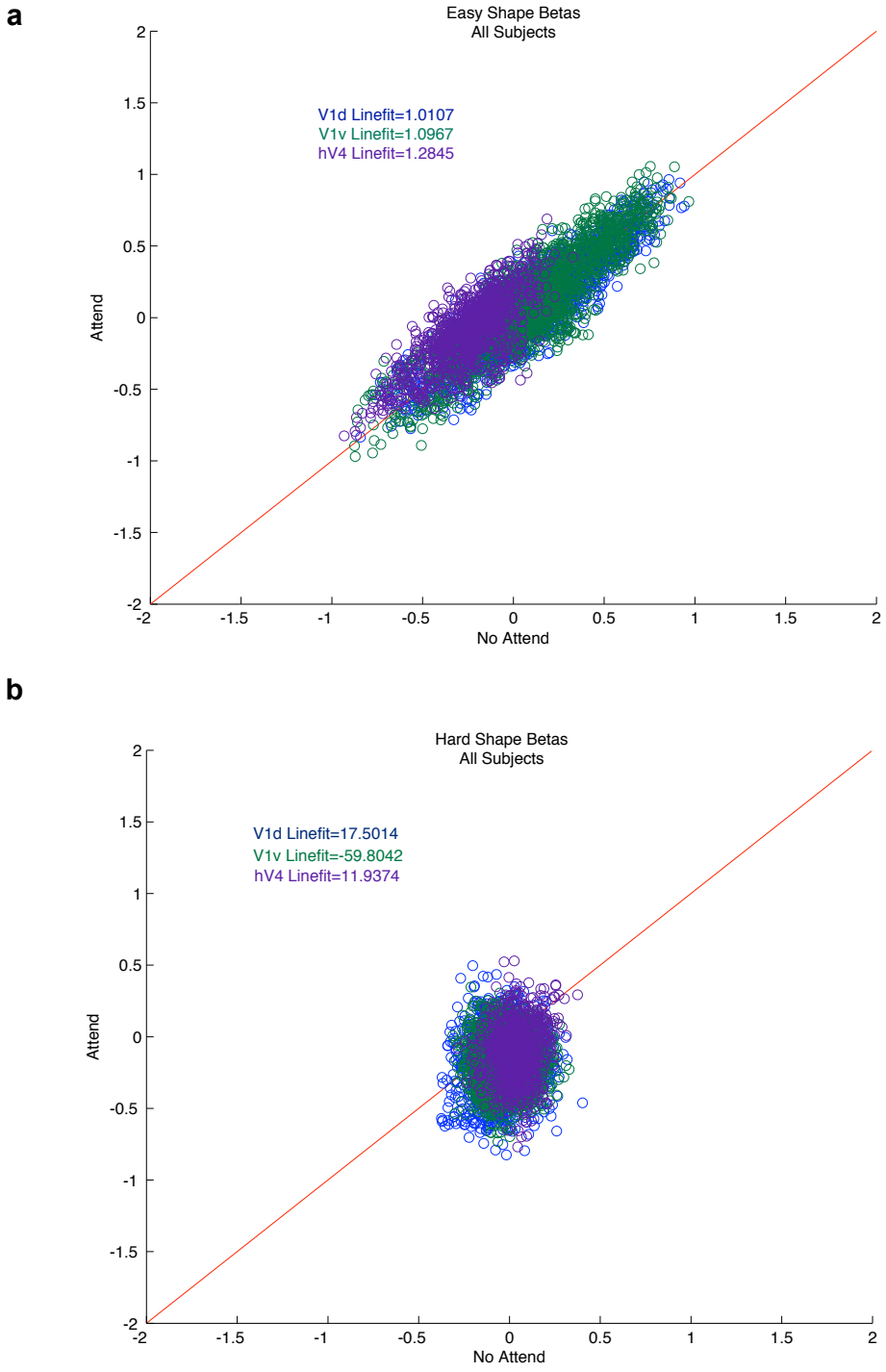

Figure 12: Attend vs no Attend State Across Subjects: a.) Attention increases shape feature beta weights in V4 but not V1d or V1v (dorsal and ventral V1, respectively) when subjects are collapsed on easy trials. The least squared line fit was 1.0 and 1.1 for V1 and V1d, and 1.3 for V4. The increase appears multiplicative. b.) There is no consistent attention or sensory effect in the hard trials when subjects are collapsed in V1 or V4; line fits are very high, and the voxels form a cloud near 0.

3.3.3 Choice Effects

We did not see strong choice effects that were clearly disassociable from the sensory effects in hard trials in V4. Line fits for all subjects were close to zero (Figure 13) (0.12, 0.05, 0.06, 0.18 for Subjects 1-4, respectively), indicating there was very little relationship between voxels which fit the shape model well and those which matched the perceptual choice well. This was likely due to the very small changes in our stimulus. Using a stimulus near threshold is necessary to disassociate sensory and choice effects so that sensory and choice are not overlapping to an extent that makes regression analysis impossible, but our design may have brought the stimulus too close to threshold, which may have resulted in a low SNR in the BOLD signal that was incapable of detecting the small changes in the stimulus. Interestingly, choice beta weights were larger in amplitude than sensory effects, suggesting that while there may not have been a strong stimulus related signal; a perceptual choice signal might still be detectable in the data.

3.3.4 Consistency of Voxels Across Easy and Hard Tasks

Due to the larger amplitude of the choice beta weights. despite small shape beta weights and low consistency between sensory and choice beta weights, we considered addressing the issues of low sensory effects in the hard trials and high overlap of sensory and choice in the easy trials, by using sensory beta weights from the easy trials and comparing them to choice beta weights from the hard trials. Since the task was the same across easy and hard trials, sensory and choice effects should be comparable across difficulties. It could be that while the SNR is too low to see large sensory effects; perceptual choice effects might still be visible. If this were the case, there might be small sensory beta weights in the hard trials that would be far lower in amplitude, but correlated, with stronger beta weights in the easy trials. We first wanted to establish whether any detectable sensory signals existed in the hard trial data, and whether these were comparable to corresponding voxels from easy trials. However, sensory shape beta weights for voxels did not have high line fits across easy and hard trials for all subjects (Figure 14), with subjects 2 and 4 having line fits below

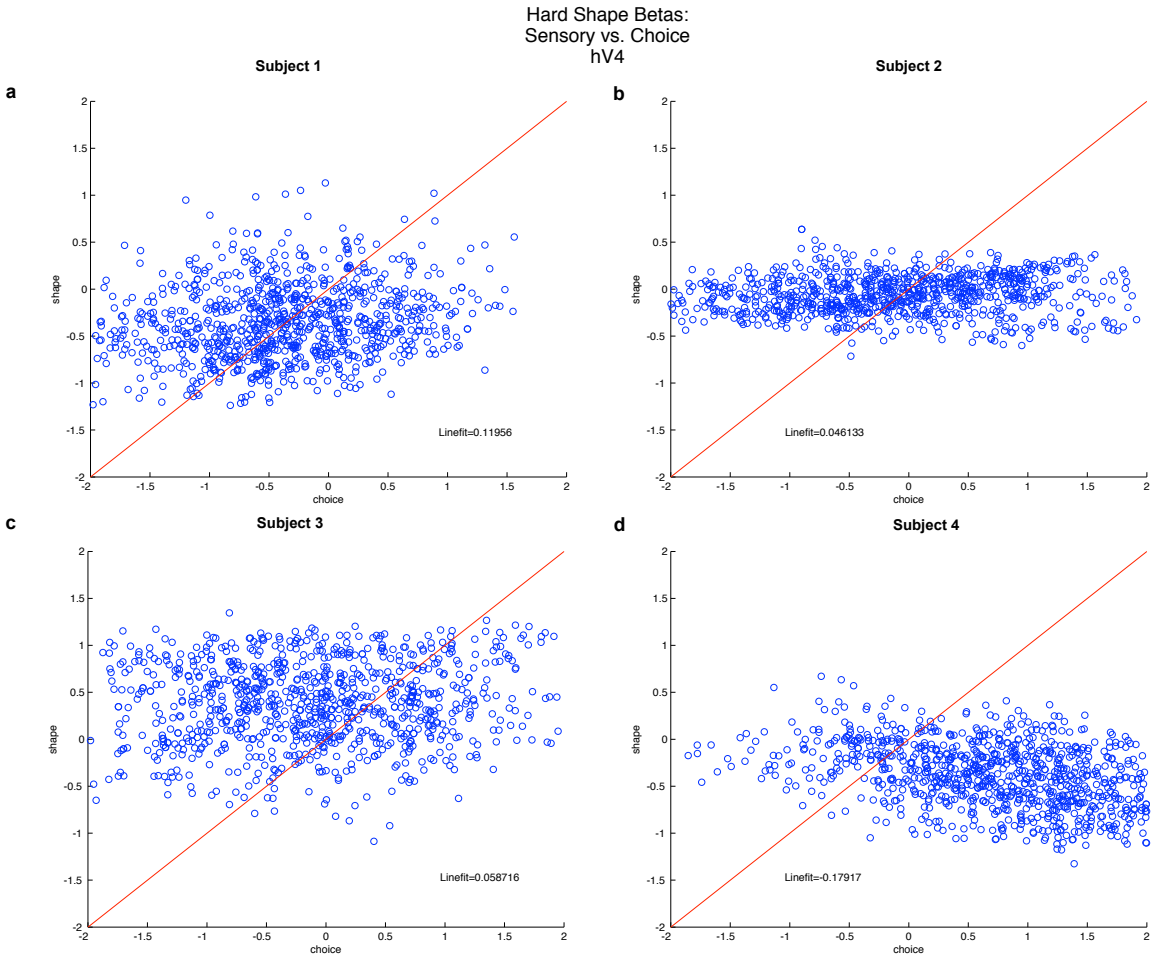

Figure 13: Choice Effects in V4: There was no consistent relationship between sensory and choice effects in V4 during hard trials for any subject (a-d). Line fits were all <0.2. Choice beta weights were twice as large as sensory beta weights, potentially implicating the presence of a reliable choice signal.

0, although subjects 1 and 3 did have line fits close to 1. B-intercepts were also close to 0, suggesting there was no additive effect due to a stronger SNR in easy trials. These results may mean that results from the hard trials do not contain a high enough SNR to be interpretable in any of the measures, at least not in all subjects. However, we reasoned that these results also could be due to the low sensory effects in the hard trials, due to the very small changes occurring in the visual stimulus, in conjunction with the presence of strong perceptual signals, especially considering the inconsistencies across subjects, and so we further analyzed the overlap between sensory and choice beta weights from easy and hard voxels, respectively.

3.3.5 Easy Attention Effects vs Hard Choice Effects

Given that choice beta weights in the hard trials (Figure 13) were larger than the sensory beta weights, it could be the case that while the SNR was too low to capture any sensory effects from such small stimulus changes, perceptual choice effects may still exist. Thus we compared attended sensory and choice effects, using attend shape beta weights from the easy trials and choice beta weights from the hard trials (Figure 15). We still did not see a consistent effect; slopes, b-intercepts, and correlation coefficients were very small, suggesting that there was not a consistent relationship between voxels high in shape attention modulations and voxels high in representations of the perceptual decision (in regards to shape).

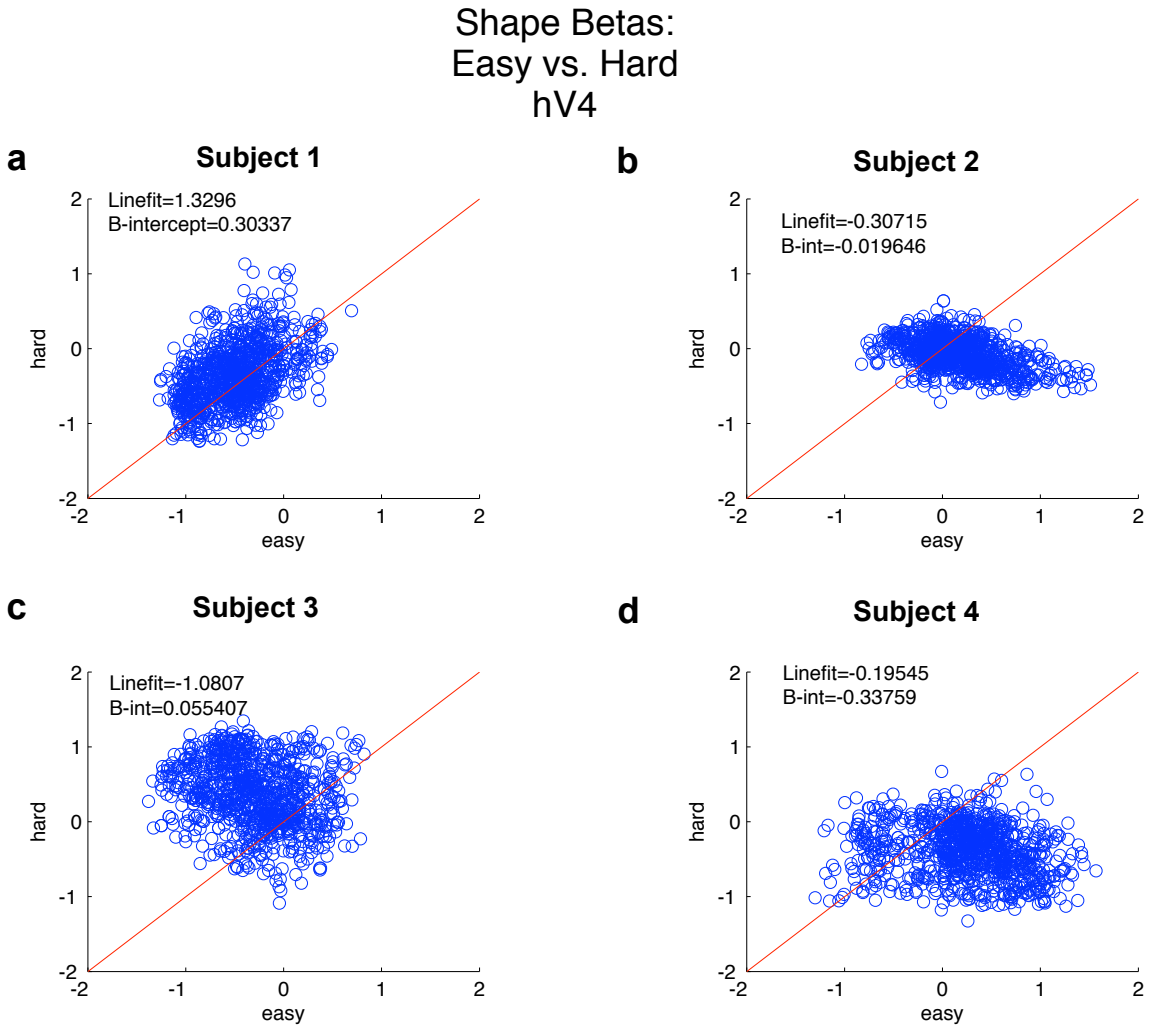

Figure 14: Voxel Stability Across Task Difficulty: Voxels were not consistent across easy and hard trials for subjects 2 and 4, with line fits near 0 (0.31 and 0.34, respectively), but were for subjects 1 and 3, with line fits near 1 (1.33 and 1.08, respectively). This suggests that sensory beta weights in hard trials are not reliable.

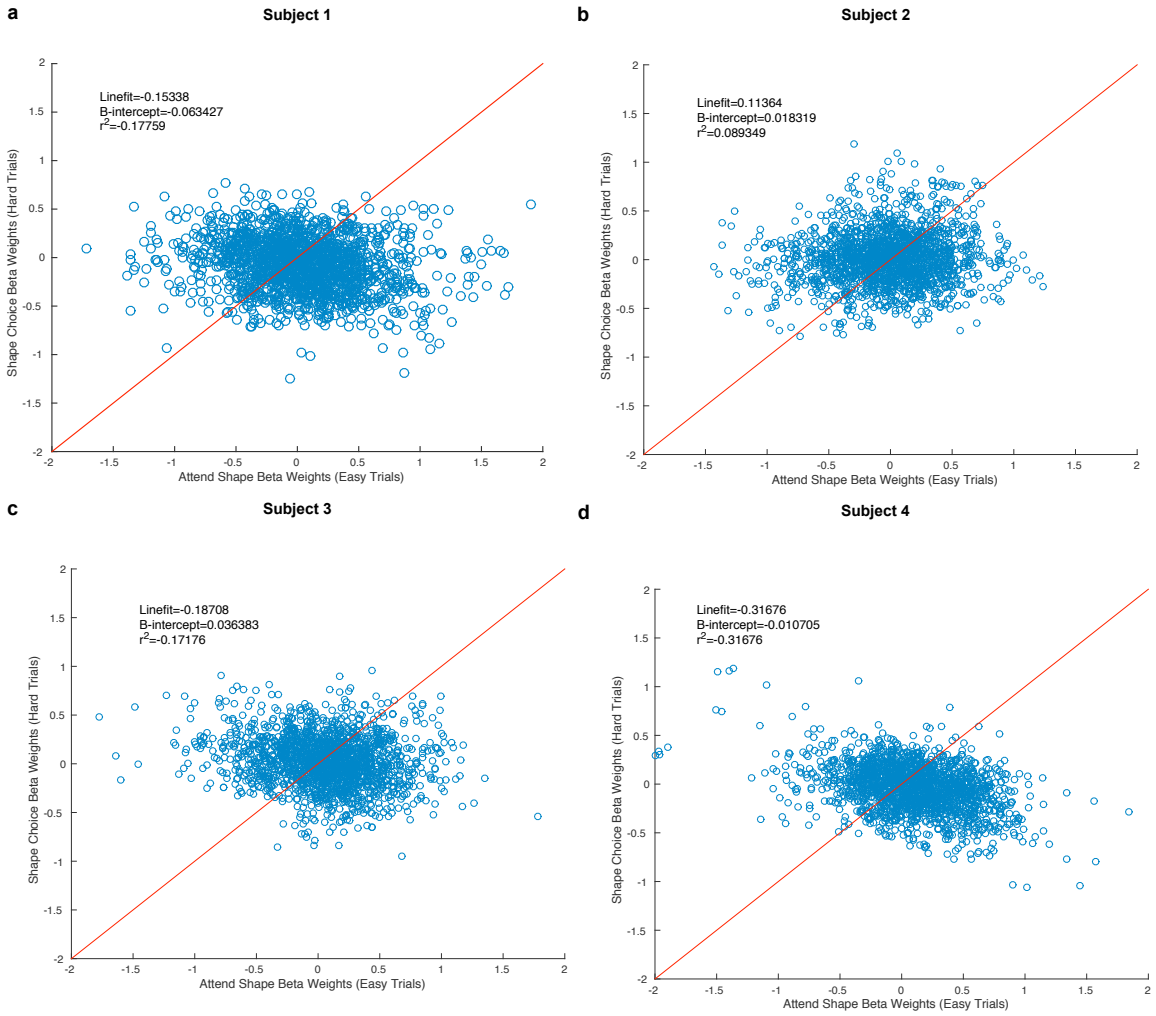

Figure 15: Attend Shape (easy) vs Choice (hard): Voxels high in attention modulations were not consistently high in choice effects for individual subjects, with the exception of a slight negative correlation for subject 4 (r^2=-0.18, 0.09, -0.17, -0.32 for subjects 1-4 respectively). B-intercepts were also near 0 for all subjects (<0.06), and line fits were near 0 for all subjects, except a small multiplicative increase for subject 4 (-0.15, 0.11, -0.19, and -0.32 for subjects 1-4, respectively)

4 Discussion

4.1 Learning

We asked whether or not, and how, neural signals, implicated in visual task performance, can explain behavioral changes during learning of that task. Employing a task in which animals were required to detect shapes degraded by noise, we found that neural population LFP signals, recorded on single microelectrodes over tens of milliseconds in V4, reliably signaled shape perception and predicted detection events. Training over a period of weeks in this task resulted in measureable improvements in detection rate, especially for the most degraded shapes. This was accompanied by comparable increases in the reliability of both sensory and choice related signals on individual electrodes. Moreover, we found that non-monotonic changes in performance, over blocks of hundreds of trials (Gureckis and Love, 2009), were highly correlated with the changes in the reliability of informative sensory signals. We conclude that V4 is involved in VPL of shapes, and the enhancement of encoding in early visual sensory signals at or before the level of V4, rather than a change in readout from higher level areas, explains fluctuations over time course of hundreds of trials.

Improvements in performance could arise from improvements in the encoding of stimuli, improvements in the readout of sensory representations, or some combination. Identifying this locus has been challenging because traditional electrophysiological analyses cannot readily separate these contributions to neural activity. For example, although average shape-aligned and saccade-aligned responses (Figure 4) increase over the course of learning, because of the temporal overlap of shape-triggered and saccade-triggered responses, it is difficult to isolate such components (Panzeri et al., 2017). Averaging faces an additional limitation, in that the ability of signals to predict behavior on a trial by trial basis is not established. We addressed such challenges by adopting a moment-to-moment approach which avoids such averages and makes use of a covariance correction to isolate sensory and choice signals (Harrison et al., 2013). We found that populations sampled by individual electrodes can reliably signal the presence of the stimulus and upcoming behavioral decision within reaction time limited windows. The distribution of task relevant information was heterogeneous across

our recording arrays; however the particular electrodes that were the most informative of the shape were also the most predictive of choices after learning.

Previous VPL studies (cf (Yan et al., 2014)) have largely relied on making comparisons between measurements made at the beginning and end of training, and not during the actual training process. With such an approach, physiological changes may reflect changes that occurred during learning, without actually being responsible for those changes. We found that both sensory and choice reliability dramatically increased over the course of learning, but fluctuations in behavior over time scales of hundreds of trials better reflect sensory, rather choice, dynamics. This seemingly conflicts with findings (Law and Gold, 2008) that changes in sensitivity with learning were not observed in an area (MT) tuned to the stimulus (motion), but were in a higher level area (LIP), and that choice probability changes in MT were likely related to improved readout. However, there are several possibilities that explain this apparent discrepancy. Learning associated increases in neuronal sensitivity to orientations (Adab and Vogels, 2011), as well as contrasts (Sanayei et al., 2018), have been found in V4, and this region may simply be more involved in learning than MT. Increased plasticity in V4 has been proposed to be due to broader inputs to V4 compared to V1 or MT (Adab and Vogels, 2011), and it is possible that reward prediction error feedback is higher in V4 than MT (Kumano and Uka, 2013). Additionally, many studies (Law and Gold, 2008; Sanayei et al., 2018) have used neural sensitivity and choice probability measures, whereas we used sensory and choice reliability from the MI analysis. Sensory reliability is a similar measure to sensitivity, although it measures the change in strength rather than change in response to differing stimuli, respectively. However, sensitivity and choice probability do not correct for covariance between the stimulus and the behavioral decision, nor do they optimize for varying binwidths and delays. Conversely, our MI analysis corrects for covariance, allows for a direct comparison across sensory, choice, and behavior, and also computes all three measures at multiple, precise time scales.

We also found that LFPs on the most reliable electrodes were 3 to 4 times more reliable than the best

individual neurons (Weiner and Ghose, 2014), but similar to most reliable neurons ensembles of 10-40 neurons (Weiner and Ghose, 2015). This was true even prior to the beginning of degraded shape training, and suggests that interneuronal correlations that might degrade performance are minimal in this task, consistent with past results finding that such correlations are largely absent (Weiner and Ghose, 2015). One possible explanation for the lack of correlations is the demanding nature of this task. As spatial attention in V4 has been shown to reduce noise correlations (Cohen and Maunsell, 2009), it is possible that the absence of such correlations in our studies reflect the consistent allocation of attention during task performance. This is still somewhat surprising, however, because the vast majority of individual cells are non-informative with regard to either shapes or saccades (Weiner and Ghose, 2014), and one might expect that, in the spatial sampling that is reflected in LFP measurements, such neurons would dominate and result in poorly informative LFPs.

However, contributions to LFP signals from sources other than action potentials may contribute to information differences between single units and LFPs. LFPs reflect not only spikes, but also intrinsic currents, calcium spikes, sub-threshold synaptic currents, and other cellular processes that alter the electrical potential in the extracellular space being recorded, but do not necessarily produce an action potential (Buzsáki et al., 2012). Irrespective of its origin, our results are consistent with recent findings of their significance towards understanding stimulus representation (Belitski et al., 2008; Montemurro et al., 2008) and complex perceptual and cognitive features (Wang et al., 2009; Rutishauser et al., 2010; Lopour et al., 2013; Rey et al., 2015). Prior studies have also found that LFPs better reflect stimulus perception in V4 than spikes (Wilke et al., 2006), and we believe that the answer to this apparent paradox is the very low levels of correlation, and near independence, of V4 neural activity in this task (Weiner and Ghose, 2015). In the absence of such correlations, population averages of purely noisy neurons should be small, leaving the LFP to be dominated by those neurons with task relevant signals. Indeed, simple models show that even with moderate amounts of interneuronal correlation ($\approx$0.1), neurons with reliable sensory information can dominate population level signals and have reliable choice information (Krause and Ghose, 2018). Our results are also con-

sistent with suggestions that LFPs have a relatively limited and have fixed spatial sampling (Xing et al., 2009; Katzner et al., 2009); nearby electrodes, spaced 400 μm apart, often displayed very different task-related signals (Figure 6), although this only occured in the MI analysis. This highlights the importance of using an analysis that measures reliability on precise timescales, particularly when using population signals such as LFPs. We did, however, find that, while task related signals differed across the array, there was a high level of redundancy (Figure 8,9), although this did not change as a function of distance up to 3 electrodes away, in the subset of electrodes we analyzed. Interestingly, correlations were highest for early sensory and late choice populations at all three distances, suggesting there might be some effect of learning on reliability redundancy that is dependent on sensory and choice. However, further work determining how redundancy and spatial dependence changes across all electrodes along the entire array, in both animals, would be useful.

Discrepancies between LFPs and single and multi-unit observations in our data also demonstrate the usefulness of LFP signals. Particularly, the presence of very strong pre-saccadic signals in the LFP (Figure 4b,5a-b), compared to single (Weiner and Ghose, 2014) and multi (Weiner and Ghose, 2015) -unit data, suggests that LFPs may contain signals not accessible by traditional spike analyses. While our study is not specifically addressing pre-saccadic signals, the fact that they represent receptive field remapping to the saccade location (Tolias et al., 2001), and are predictive rather than representative, thus involving feedback (Sun and Goldberg, 2016; Binda and Morrone, 2018), suggests that LFPs may contain more information regarding top down influences compared to spikes. LFPs have also been found to contain natural stimulus information that is decoupled from spikes and multi-units (Belitski et al., 2008). Thus, past work, combined with our evidence that LFPs do clearly represent the stimulus and predict the decision, and that the former predicts point to point fluctuations with learning, demonstrates that LFPs are a highly informative and powerful tool in linking findings in humans and macaques. Ultimately, studying LFPs may greatly improve our understanding of how both sensory and choice related neural signal changes in populations, may underlie changes in visual perceptual performance. While LFPs have often been studied in terms of oscillations, we demonstrate their

potential in understanding trial to trial, and even moment to moment, neural changes in relation to behavior and learning, possibly representing top down influences such as pre-saccadic signals more robustly than pools of spikes. In addition to providing insight into how signals from a small number of informative sensory neurons may still be extracted from a very large pool, LFP signals may also link the human and macaque literature, and possibly provide an explanation for how BOLD signals can demonstrate learning related changes, despite sampling large pools of neurons.

Our findings that LFPs are heterogeneous and can be used to study temporally precise sensory and choice related information is consistent with previous studies establishing that, despite its spatial imprecision (Histed et al., 2009), electrical microstimulation can be used to selectively target decision relevant populations (Cohen and Newsome, 2004). Because we document changes at the level of LFPs with learning, this opens up the possibility of using microstimulation for a causative approach to the study of VPL. For example, experiments involving repetitive stimulation during perceptual training might be capable of establishing whether localized activity fluctuations are sufficient for learning. Our study suggests that V4, by containing reliable and decision predictive signals which increase during the course of learning, would be a promising target for such an approach with respect to shape learning.

4.2 Attention

With the experimental design and analysis approach we used, we were not able to clearly determine if attention and choice signals are disassociable, using fMRI on a single voxel level, and so we were unable to answer the question of whether individual voxels, that are highly modulated by attention to a shape stimulus, also carry high perceptual shape choice signals. While even a comparison across easy and hard trials did not show consistent correlations between voxels modulated by attention to shape and those modulated by a shape related decision, there was a slight negative correlation for subject 4 (r^2=-0.32), which could imply that voxels tuned to an attended stimulus are suppressed in order to make a decision. However, given that this

was not consistent across subjects, we cannot make such a conclusion. We also found that b-intercepts were low, suggesting that there is not an additive effect of attention or choice, although again, this is difficult to confirm given the lack of consistent results in the hard trials. However, we did confirm that attention effects are increased in a multiplicative manner in V4 for shapes, but not in V1, using the easy trial data, and this can be seen on an individual voxel level at high resolution.

The inability to disassociate sensory and choice signals is likely due to the experimental design combined with the use of fMRI imaging. While these results could also suggest that the same voxels do not carry sensory and choice signals, we cannot rule out that it is because sensory and choice signals were not sufficiently disassociated, methodologically. Our results are, however, unlikely to be due to an instability in voxels over runs, given that easy and hard voxels were consistent across runs within a difficulty, and two subjects were even consistent across difficulty (Figure 14). More likely, the problem is due to an issue of low SNR. BOLD signals have low SNR due to high amounts of noise associated with fMRI scanning, and our hard trials may have pushed the subject too close to a stimulus and/or perceptual threshold to determine such effects, although it does appear that perceptual effects may exist, given the large hard choice beta weights Figure (15). But this cannot be definitively concluded when they do not overlap with sensory results from the easy trials. However, our easy trials had too much overlap between the perceptual report and the stimulus in order to disassociate signals as slow as BOLD, given near perfect performance in the easy trials, to compare sensory/attention beta weights with choice beta weights. Even when we attempted to use sensory/attention beta weights from the easy trials and compare them to choice beta weights with the hard trials, there was not a consistent relationship across subjects (Figure 15.

One potential solution to these issues would be to use an array of difficulties per subject to determine at what difficulty threshold sensory effects are visible, rather than only utilizing a single pre-test of performance, and then use the most optimal difficulty to disassociate sensory and choice signals. An increase in subject number would also likely be beneficial, given that two subjects did show overlap in shape betas between easy

and hard trials and one subject did show a slight negative correlation between easy attention and hard choice beta weights. Additionally, this task could be used in nonhuman primates with electrophysiology techniques, where temporal and spatial resolution is far higher. Given that we can see attentional effects on individual voxels in V4, it is likely that attention and choice effects could be disassociated, given an increased number of subjects in conjunction with more subject-specific optimized task parameters.

4.3 Conclusion: Visual Perception and Future Directions

Separating the effects of the stimulus and the behavioral choice is integral to understanding visual perception. If we want to understand how humans and other animals perceive the world around them, and how neural substrates change in conjunction with changes in perception, it is necessary to disassociate changes in sensory and choice effects over small and large time scales. This is not a trivial issue, given the fast timescales on which perceptual decisions are made. However, using a variety of tools, models, subjects, and brain signals, we may be able to better understand how the brain alters neural signaling to enable improvements in behavior.

Our work demonstrates that for perceptual learning, changes in sensory encoding best explain long term improvements in behavior in area V4. Additionally, on short timescales, the same neurons that signal the sensory event, also signal the perceptual report, and the relationship between populations, in measures of sensory and choice, stays consistent over weeks of learning. Thus it is likely, that on the short time scales of attention, this relationship would also hold true. However, we were not able to determine the overlap between attentional and choice signals with the attention experiment. Further work is necessary to understand how neurons in V4 change with attention in relationship to their choice reliability, as well as causal work to determine the necessity of V4 signals in both attention and learning. However, these studies do suggest that sensory representations in V4 mediate long term learning, as well as explain short term changes in both attention and perceptual decisions.

References

Abernethy, B., Schorer, J., Jackson, R. C., and Hagemann, N. (2012). Perceptual training methods compared: The relative efficacy of different approaches to enhancing sport-specific anticipation. *Journal of Experimental Psychology: Applied*, 18(2):143–153.

Adab, H. Z. and Vogels, R. (2011). Practicing coarse orientation discrimination improves orientation signals in macaque cortical area v4. *Current biology : CB*, 21(19):1661–6.

Ahissar, M. and Hochstein, S. (1993). Attentional control of early perceptual learning. *Proceedings of the National Academy of Sciences of the United States of America*, 90(12):5718–22.

Ahissar, M. and Hochstein, S. (1997). Task difficulty and the specificity of perceptual learning. *Letters to Nature*, 387:401–406.

Ahissar, M. and Hochstein, S. (2004). The reverse hierarchy theory of visual perceptual learning. *Trends in Cognitive Sciences*, 8(10):457–464.

Anton-Erxleben, K. and Carrasco, M. (2013). Attentional enhancement of spatial resolution: Linking behavioural and neurophysiological evidence. *Nature Reviews Neuroscience*, 14(3):188–200.

Anton-Erxleben, K., Stephan, V. M., and Treue, S. (2009). Attention reshapes center-surround receptive field structure in macaque cortical area MT. *Cerebral Cortex*, 19(10):2466–2478.

Arcizet, F., Jouffrais, C., and Girard, P. (2008). Natural textures classification in area V4 of the macaque monkey. *Experimental Brain Research*, 189(1):109–120.

Arcizet, F., Mirpour, K., Foster, D. J., and Bisley, J. W. (2018). Activity in LIP, but not V4, matches performance when attention is spread. *Cerebral Cortex*, 28(12):4195–4209.

Arman, A. C., Ciaramitaro, V. M., and Boynton, G. M. (2006). Effects of feature-based attention on the motion aftereffect at remote locations. *Vision Research*, 46(18):2968–2976.

Baldassarre, A., Lewis, C. M., Committeri, G., Snyder, A. Z., Romani, G. L., and Corbetta, M. (2012). Individual variability in functional connectivity predicts performance of a perceptual task. *Proceedings of the National Academy of Sciences*, 109(9):3516–3521.

Bao, M., Yang, L., Rios, C., He, B., and Engel, S. a. (2010). Perceptual learning increases the strength of the earliest signals in visual cortex. *The Journal of neuroscience : the official journal of the Society for Neuroscience*, 30(45):15080–15084.

Barbot, A. and Carrasco, M. (2017). Attention Modifies Spatial Resolution According to Task Demands. *Psychological Science*, 28(3):285–296.

Bartsch, M. V., Donohue, S. E., Strumpf, H., Schoenfeld, M. A., and Hopf, J.-M. (2018). Enhanced spatial focusing increases feature-based selection in unattended locations. *Scientific Reports*, 8(1):1–14.

Beauregard, M. and Lévesque, J. (2006). Functional magnetic resonance imaging investigation of the effects of neurofeedback training on the neural bases of selective attention and response inhibition in children with attention-deficit/hyperactivity disorder. *Applied Psychophysiology Biofeedback*, 31(1):3–20.

Bejjanki, V. R., Beck, J. M., Lu, Z.-L., and Pouget, A. (2011). Perceptual learning as improved probabilistic inference in early sensory areas. *Nature neuroscience*, 14(5):642–648.

Belitski, A., Gretton, A., Magri, C., Murayama, Y., Montemurro, M. A., Logothetis, N. K., and Panzeri, S. (2008). Low-Frequency Local Field Potentials and Spikes in Primary Visual Cortex Convey Independent Visual Information. *Journal of Neuroscience*, 28(22):5696–5709.

Binda, P. and Morrone, M. C. (2018). Vision During Saccadic Eye Movements. *Annual Review of Vision Science*, 4:193–213.

Burton, a. M., Wilson, S., Cowan, M., and Bruce, V. (1999). FACE RECOGNITION IN POOR-QUALITY VIDEO: Evidence From Security Surveillance. *Psychological Science*, 10(3):243–248.

Buzsáki, G., Anastassiou, C. A., and Koch, C. (2012). The origin of extracellular fields and currents-EEG, ECoG, LFP and spikes. *Nature Reviews Neuroscience*, 13(6):407–420.

Byers, A. and Serences, J. T. (2012). Exploring the relationship between perceptual learning and top-down attentional control. *Vision Research*, 74:30–39.

Byers, A. and Serences, J. T. (2014). Enhanced attentional gain as a mechanism for generalized perceptual learning in human visual cortex. *Journal of Neurophysiology*, 112:1217–1227.

Carlson, E. T., Rasquinha, R. J., Zhang, K., and Connor, C. E. (2011). A sparse object coding scheme in area V4. *Current Biology*, 21(4):288–293.

Carrasco, M. (2011). Visual attention: The past 25 years. *Vision Research*, 51:1484–1525.

Carrasco, M. and Barbot, A. (2019). Spatial attention alters visual appearance. *Current Opinion in Psychology*, 29:56–64.

Carrasco, M., Ling, S., and Read, S. (2004). Attention Alters Appearance. *Nature Neuroscience*, 7(3):79–106.

Choe, K. W., Blake, R., and Lee, S.-H. (2014). Dissociation between Neural Signatures of Stimulus and Choice in Population Activity of Human V1 during Perceptual Decision-Making. *Journal of Neuroscience*, 34(7):2725–2743.

Chung, S. T., Legge, G. E., and Cheung, S. H. (2004). Letter-recognition and reading speed in peripheral vision benefit from perceptual learning. *Vision Research*, 44(7):695–709.

Churchland, M. M., Yu, B. M., Cunningham, J. P., Sugrue, L. P., Cohen, M. R., Corrado, G. S., Newsome, W. T., Clark, A. M., Hosseini, P., Scott, B. B., Bradley, D. C., Smith, M. A., Kohn, A., Movshon, J. A., Armstrong, K. M., Moore, T., Chang, S. W., Snyder, L. H., Lisberger, S. G., Priebe, N. J., Finn, I. M.,

Ferster, D., Ryu, S. I., Santhanam, G., Sahani, M., and Shenoy, K. V. (2010). Stimulus onset quenches neural variability: a widespread cortical phenomenon. *Nature Neuroscience*, 13(3):369–378.

Cohen, M. R. and Maunsell, J. H. (2009). Attention improves performance primarily by reducing interneuronal correlations. *Nature Neuroscience*, 12(12):1594–1600.

Cohen, M. R. and Newsome, W. T. (2004). What electrical microstimulation has revealed about the neural basis of cognition. *Current Opinion in Neurobiology*, 14(2):169–177.

Cohen, M. R. and Newsome, W. T. (2009). Estimates of the Contribution of Single Neurons to Perception Depend on Timescale and Noise Correlation. *Journal of Neuroscience*, 29(20):6635–6648.

Cortese, S., Ferrin, M., Brandeis, D., Buitelaar, J., Daley, D., Dittmann, R. W., Holtmann, M., Santosh, P., Stevenson, J., Stringaris, A., Zuddas, A., and Sonuga-Barke, E. J. (2015). Cognitive Training for Attention-Deficit/Hyperactivity Disorder: Meta-Analysis of Clinical and Neuropsychological Outcomes From Randomized Controlled Trials. *Journal of the American Academy of Child & Adolescent Psychiatry*, 54(3):164–174.

Cox, M. A., Schmid, M. C., Peters, A. J., Saunders, R. C., Leopold, D. A., and Maier, A. (2013). Receptive field focus of visual area V4 neurons determines responses to illusory surfaces. *Proceedings of the National Academy of Sciences*, 110(42):17095–17100.

Cumming, B. G. and Nienborg, H. (2016). Feedforward and feedback sources of choice probability in neural population responses. *Current Opinion in Neurobiology*, 37:126–132.

Cutzu, F. and Tsotsos, J. K. (2003). The selective tuning model of attention: Psychophysical evidence for a suppressive annulus around an attended item. *Vision Research*, 43(2):205–219.

David, S. V., Hayden, B. Y., Mazer, J. A., and Gallant, J. L. (2008). Attention to Stimulus Features Shifts Spectral Tuning of V4 Neurons during Natural Vision. *Neuron*, 59(3):509–521.

Denker, M., Roux, S., Lindén, H., Diesmann, M., Riehle, A., and Grün, S. (2011). The local field potential reflects surplus spike synchrony. *Cerebral Cortex*, 21(12):2681–2695.

Dosher, B. A. and Lu, Z.-L. (1998). Perceptual learning reflects external noise filtering and internal noise reduction through channel reweighting. *Proceedings of the National Academy of Sciences*, 95(23):13988–13993.

Dosher, B. A. and Lu, Z. L. (1999). Mechanisms of perceptual learning. *Vision Research*, 39:3197–3221.

Engel, S. A., Christopher, F. S., and Schluppeck, D. (2004). Learning Strengthens the Response of Primary Visual Cortex to Simple Patterns. *Current Biology*, 14:573–578.

Epstein, J. N., Conners, C. K., Erhardt, D., March, J. S., and Swanson, J. M. (1997). Asymmetrical Hemispheric Control of Visual-Spatial Attention in Adults With Attention Deficit Hyperactivity Disorder quite inconsistent in the degree to which they discriminate. *Neuropsychology*, 11(4):467–473.

Fahle, M. (2004). Perceptual learning: a case for early selection. *Journal of vision*, 4(10):879–890.

Gadgil, M., Peterson, E., Tregellas, J., Hepburn, S., and Rojas, D. (2013). Differences in global and local level information processing in autism: an fMRI investigation. *Psychiatry Res*, 213(2):115–121.

Gattass, R., Galkin, T. W., Desimone, R., and Ungerleider, L. G. (2014). Subcortical connections of area V4 in the macaque. *Journal of Comparative Neurology*, 522(8):1941–1965.

Ghose, G. M. (2006). Strategies optimize the detection of motion transients. *Journal of Vision*, 6(4):10.

Ghose, G. M. (2009). Attentional Modulation of Visual Responses by Flexible Input Gain. *Journal of Neurophysiology*, 101(4):2089–2106.

Ghose, G. M. and Bearl, D. W. (2010). Attention directed by expectations enhances receptive fields in cortical area MT. *Vision Research*, 50(4):441–451.

Ghose, G. M. and Harrison, I. T. (2009). Temporal precision of neuronal information in a rapid perceptual judgment. *Journal of neurophysiology*, 101(3):1480–93.

Ghose, G. M. and Maunsell, J. H. R. (2008). Spatial Summation Can Explain the Attentional Modulation of Neuronal Responses to Multiple Stimuli in Area V4. *Journal of Neuroscience*, 28(19):5115–5126.

Ghose, G. M., Yang, T., and Maunsell, J. H. R. (2002). Physiological correlates of perceptual learning in monkey V1 and V2. *Journal of neurophysiology*, 87(4):1867–1888.

Gobell, J. and Carrasco, M. (2005). Attention Alters the Appearance of Spatial Frequency and Gap Size. *Psychological Science*, 16(8):644–651.

Goense, J. B. M. and Logothetis, N. K. (2008). Neurophysiology of the BOLD fMRI Signal in Awake Monkeys. *Current Biology*, 18(9):631–640.

Goris, R. L., Ziemba, C. M., Stine, G. M., Simoncelli, E. P., and Movshon, J. A. (2017). Dissociation of Choice Formation and Choice-Correlated Activity in Macaque Visual Cortex. *The Journal of Neuroscience*, 37(20):5195–5203.

Gottlieb, J. P., Kusunoki, M., and Goldberg, M. E. (1998). The representation of visual salience in monkey parietal cortex. *Nature*, 391(6666):481–484.

Greenwood, P. M., Parasuraman, R., and Alexander, G. E. (1997). Controlling the focus of spatial attention during visual search: Effects of advanced aging and Alzheimer disease. *Neuropsychology*, 11(1):3–12.

Gu, Y., Liu, S., Fetsch, C. R., Yang, Y., Fok, S., Sunkara, A., DeAngelis, G. C., and Angelaki, D. E. (2011). Perceptual learning reduces interneuronal correlations in macaque visual cortex. *Neuron*, 71(4):750–761.

Gureckis, T. M. and Love, B. C. (2009). Learning in Noise: Dynamic Decision-Making in a Variable Environment. *Journal of Mathematical Psychology*, 53(3):180–193.

Harrison, I. T., Weiner, K. F., and Ghose, G. M. (2013). Inattention Blindness to Motion in Middle Temporal Area. *Journal of Neuroscience*, 33(19):8396–8410.

Histed, M. H., Bonin, V., and Reid, R. C. (2009). Direct Activation of Sparse, Distributed Populations of Cortical Neurons by Electrical Microstimulation. *Neuron*, 63(4):508–522.

Hopf, J.-M. (2006). The Neural Site of Attention Matches the Spatial Scale of Perception. *Journal of Neuroscience*, 26(13):3532–3540.

Huang, C.-B., Zhou, Y., and Lu, Z.-L. (2008). Broad bandwidth of perceptual learning in the visual system of adults with anisometropic amblyopia. *Proceedings of the National Academy of Sciences of the United States of America*, 105(10):4068–73.

Hung, S.-C. and Seitz, A. R. (2014). Prolonged Training at Threshold Promotes Robust Retinotopic Specificity in Perceptual Learning. *Journal of Neuroscience*, 34(25):8423–8431.

Jeanne, J. M., Sharpee, T. O., and Gentner, T. Q. (2013). Associative learning enhances population coding by inverting interneuronal correlation patterns. *Neuron*, 78(2):352–363.

Jehee, J. F. M., Ling, S., Swisher, J. D., van Bergen, R. S., and Tong, F. (2012). Perceptual Learning Selectively Refines Orientation Representations in Early Visual Cortex. *Journal of Neuroscience*, 32(47):16747–16753.

Jeter, P. E., Dosher, B. A., Petrov, A., and Lu, Z.-L. (2009). Task precision at transfer determines specificity of perceptual learning. *Journal of Vision*, 9(3):1–13.

Joiner, W. M., Cavanaugh, J., and Wurtz, R. H. (2011). Modulation of shifting receptive field activity in frontal eye field by visual salience. *Journal of Neurophysiology*, 106(3):1179–1190.

Kajikawa, Y. and Schroeder, C. E. (2011). How local is the local field potential? *Neuron*, 72(5):847–858.

Kajikawa, Y. and Schroeder, C. E. (2014). Generation of field potentials and modulation of their dynamics through volume integration of cortical activity. *Journal of Neurophysiology*, 113(1):339–351.

Kanashiro, T., Ocker, G. K., Cohen, M. R., and Doiron, B. (2017). Attentional modulation of neuronal variability in circuit models of cortex. *eLife*, 6:1–38.

Karni, a. and Sagi, D. (1991). Where practice makes perfect in texture discrimination: evidence for primary visual cortex plasticity. *Proceedings of the National Academy of Sciences of the United States of America*, 88(11):4966–4970.

Katzner, S., Nauhaus, I., Benucci, A., Bonin, V., Ringach, D. L., and Carandini, M. (2009). Local Origin of Field Potentials in Visual Cortex. *Neuron*, 61(1):35–41.

Kellman, P. J., Massey, C. M., and Son, J. Y. (2010). Perceptual learning modules in mathematics: Enhancing students' pattern recognition, structure extraction, and fluency. *Topics in Cognitive Science*, 2(2):285–305.

Kirsch, W., Heitling, B., and Kunde, W. (2018). Changes in the size of attentional focus modulate the apparent object's size. *Vision Research*, 153(March):82–90.

Kobatake, E. and Tanaka, K. (1994). Neuronal Selectivities to Complex Object Features in the Ventral Visual Pathway of the Macaque Cerebral Cortex. *Journal of Neurophysiology*, 71(3):856–867.

Kosai, Y., El-Shamayleh, Y., Fyall, A. M., and Pasupathy, A. (2014). The role of visual area v4 in the discrimination of partially occluded shapes. *The Journal of neuroscience : the official journal of the Society for Neuroscience*, 34(25):8570–84.

Kourtzi, Z., Betts, L. R., Sarkheil, P., and Welchman, A. E. (2005). Distributed neural plasticity for shape learning in the human visual cortex. *PLoS Biology*, 3(7):1317–1327.

Krause, B. M. and Ghose, G. M. (2018). Micropools of reliable area MT neurons explain rapid motion detection. *Journal of Neurophysiology*, 120(5):2396–2409.

Kumano, H. and Uka, T. (2013). Neuronal mechanisms of visual perceptual learning. *Behavioural Brain Research*, 249:75–80.

Law, C. T. and Gold, J. I. (2008). Neural correlates of perceptual learning in a sensory-motor, but not a sensory, cortical area. *Nature Neuroscience*, 11:505–513.

Law, C. T. and Gold, J. I. (2010). Shared mechanisms of perceptual learning and decision making. *Topics in Cognitive Science*, 2(2):226–238.

Le Dantec, C. C. and Seitz, A. R. (2012). High resolution, high capacity, spatial specificity in perceptual learning. *Frontiers in Psychology*, 3:1–7.

Lennie, P. (2003). Primer - Receptive fields. *Current Biology*, 13(6):R216–R219.

Li, R., Polat, U., Makous, W., and Bavelier, D. (2009). Enhancing the contrast sensitivity function through action video game training. *Nature neuroscience*, 12(5):549–551.

Li, W. (2016). Perceptual Learning: Use-Dependent Cortical Plasticity. *Annual Review of Vision Science*, 2(1):109–130.

Li, W., Piëch, V., and Gilbert, C. D. (2004). Perceptual learning and top-down influences. *Nature Neuroscience*, 7(6):651–657.

Liu, T. and Mance, I. (2011). Constant spread of feature-based attention across the visual field. *Vision Research*, 51(1):26–33.

Liu, T., Stevens, S. T., and Carrasco, M. (2007). Comparing the time course and efficacy of spatial and feature-based attention. *Vision Research*, 47(1):108–113.

Logothetis, N. K., Pauls, J., Augath, M., Trinath, T., and Oeltermann, A. (2001). Neurophysiological investigation of the basis of the fMRI signal. *Nature*, 412(6843):150–157.

Lopour, B. A., Tavassoli, A., Fried, I., and Ringach, D. L. (2013). Coding of information in the phase of local field potentials within human medial temporal lobe. *Neuron*, 79(3):594–606.

Manning, J. R., Jacobs, J., Fried, I., and Kahana, M. J. (2009). Broadband Shifts in Local Field Potential Power Spectra Are Correlated with Single-Neuron Spiking in Humans. *The Journal of Neuroscience*, 29(43):13613–13620.

Marino, A. C. and Mazer, J. A. (2018). Saccades Trigger Predictive Updating of Attentional Topography in Area V4. *Neuron*, 98(2):429–438.

Maunsell, J. H. and Cook, E. P. (2002). The role of attention in visual processing. *Philosophical Transactions of the Royal Society B: Biological Sciences*, 357(1424):1063–1072.

Mazer, B. L., Sofer, S., Korner-Bitensky, N., Gelinas, I., Hanley, J., and Wood-Dauphinee, S. (2003). Effectiveness of a visual attention retraining program on the driving performance of clients with stroke. *Archives of Physical Medicine and Rehabilitation*, 84(4):541–550.

McAdams, C. J. and Maunsell, J. H. (2000). Attention to both space and feature modulates neuronal responses in macaque area V4. *Journal of neurophysiology*, 83(3):1751–5.

McGovern, D. P., Webb, B. S., and Peirce, J. W. (2012). Transfer of perceptual learning between different visual tasks. *Journal of Vision*, 12(11):4–4.

McMains, S. A., Fehd, H. M., Emmanouil, T.-A., and Kastner, S. (2007). Mechanisms of Feature- and Space-Based Attention: Response Modulation and Baseline Increases. *Journal of Neurophysiology*, 98(4):2110–2121.

Medalia, A., Aluma, M., Tryon, W., and Merriam, A. E. (1998). Effectiveness of attention training in schizophrenia. *Schizophrenia Bulletin*, 24(1):147–152.

Mineault, P. J., Zanos, T. P., and Pack, C. C. (2013). Local field potentials reflect multiple spatial scales in V4. *Frontiers in computational neuroscience*, 7(21):1–15.

Montemurro, M. A., Rasch, M. J., Murayama, Y., Logothetis, N. K., and Panzeri, S. (2008). Phase-of-Firing Coding of Natural Visual Stimuli in Primary Visual Cortex. *Current Biology*, 18(5):375–380.

Moran, J. and Desimone, R. (1985). Selective Attention Gates Visual Processing in the Extrastriate Cortex Author (s): Jeffrey Moran and Robert Desimone Published by : American Association for the Advancement of Science Stable URL : http://www.jstor.org/stable/1696121. *Science*, 229(4715):782–784.

Motter, B. C. (1993). Focal attention produces spatially selective processing in visual cortical areas V1, V2, and V4 in the presence of competing stimuli. *Journal of neurophysiology*, 70(3):909–19.

Motter, B. C. (2009). Central V4 Receptive Fields Are Scaled by the V1 Cortical Magnification and Correspond to a Constant-Sized Sampling of the V1 Surface. *Journal of Neuroscience*, 29(18):5749–5757.

Nazir, T. A., Ben-Boutayab, N., Decoppet, N., Deutsch, A., and Frost, R. (2004). Reading habits, perceptual learning, and recognition of printed words. *Brain and Language*, 88(3):294–311.

Neupane, S., Guitton, D., and Pack, C. C. (2016a). Dissociation of forward and convergent remapping in primate visual cortex. *Current Biology*, 26(12):R491–R492.

Neupane, S., Guitton, D., and Pack, C. C. (2016b). Two distinct types of remapping in primate cortical area V4. *Nature Communications*, 7:1–11.

Ni, A. M., Ruff, D. A., Alberts, J. J., Symmonds, J., and Cohen, M. R. (2018). Learning and attention reveal a general relationship between neuronal variability and perception. *Science*, 465(January):1–28.

Nienborg, H. and Cumming, B. G. (2006). Macaque V2 Neurons, But Not V1 Neurons, Show Choice-Related Activity. *Journal of Neuroscience*, 26(37):9567–9578.

Nienborg, H. and Cumming, B. G. (2009). Decision-related activity in sensory neurons reflects more than a neuron's causal effect. *Nature*, 459(7243):89–92.

Palmer, C., Cheng, S.-Y., and Seidemann, E. (2007). Linking Neuronal and Behavioral Performance in a Reaction-Time Visual Detection Task. *Journal of Neuroscience*, 27(30):8122–8137.

Panzeri, S., Harvey, C. D., Piasini, E., Latham, P. E., and Fellin, T. (2017). Cracking the Neural Code for Sensory Perception by Combining Statistics, Intervention, and Behavior. *Neuron*, 93(3):491–507.

Parker, A. J. and Newsome, W. T. (1998). SENSE AND THE SINGLE NEURON: Probing the Physiology of Perception. *Annual Review of Neuroscience*, 21(1):227–277.

Pasupathy, a. and Connor, C. E. (2001). Shape representation in area V4: position-specific tuning for boundary conformation. *Journal of neurophysiology*, 86(5):2505–2519.

Petrov, A. A., Dosher, B. A., and Lu, Z. L. (2005). The dynamics of perceptual learning: An incremental reweighting model. *Psychological Review*, 112(4):715–743.

Poort, J., Khan, A. G., Pachitariu, M., Nemri, A., Orsolic, I., Krupic, J., Bauza, M., Sahani, M., Keller, G. B., Mrsic-Flogel, T. D., and Hofer, S. B. (2015). Learning Enhances Sensory and Multiple Non-sensory Representations in Primary Visual Cortex. *Neuron*, 86(6):1478–1490.

Posner, M. and Cohen, Y. (1984). Components of visual orienting. *Attention and performance*, pages 531–556.

Raiguel, S., Vogels, R., Mysore, S. G., and Orban, G. a. (2006). Learning to see the difference specifically alters the most informative V4 neurons. *The Journal of neuroscience : the official journal of the Society for Neuroscience*, 26(24):6589–602.

Rainer, G., Lee, H., and Logothetis, N. K. (2004). The effect of learning on the function of monkey extrastriate visual cortex. *PLoS biology*, 2(2):E44.

Rasch, M. J., Gretton, A., Murayama, Y., Maass, W., and Logothetis, N. K. (2008). Inferring Spike Trains From Local Field Potentials. *Journal of Neurophysiology*, 99(3):1461–1476.

Rey, H. G., Ahmadi, M., and Quian Quiroga, R. (2015). Single trial analysis of field potentials in perception, learning and memory. *Current Opinion in Neurobiology*, 31:148–155.

Ritchie, K. L. and Burton, A. M. (2016). Learning faces from variability. *Quarterly Journal of Experimental Psychology*, 70(5):897–905.

Robertson, C. E., Kravitz, D. J., Freyberg, J., Baron-Cohen, S., and Baker, C. I. (2013). Tunnel Vision: Sharper Gradient of Spatial Attention in Autism. *Journal of Neuroscience*, 33(16):6776–6781.

Roe, A. W., Chelazzi, L., Connor, C. E., Conway, B. R., Fujita, I., Gallant, J. L., Lu, H., and Vanduffel, W. (2012). Toward a Unified Theory of Visual Area V4. *Neuron*, 74(1):12–29.

Romo, R., Hernandez, A., and Zainos, A. (2004). Neuronal Correlates of a Perceptual Decision in Ventral Premotor Cortex. *Neuron*, 41:165–173.

Ruff, D. A. and Cohen, M. R. (2016). Attention Increases Spike Count Correlations between Visual Cortical Areas. *Journal of Neuroscience*, 36(28):7523–7534.

Rutishauser, U., Ross, I. B., Mamelak, A. N., and Schuman, E. M. (2010). Human memory strength is predicted by theta-frequency phase-locking of single neurons. *Nature*, 464(7290):903–907.

Saenz, M., Buracas, G. T., and Boynton, G. M. (2002). Global effects of feature-based attention in human visual cortex. *Nature Neuroscience*, 5(7):631–632.

Sagi, D. (2011). Perceptual learning in Vision Research. *Vision Research*, 51(13):1552–1566.

Sanayei, M., Chen, X., Chicharro, D., Distler, C., Panzeri, S., and Thiele, A. (2018). Perceptual learning of fine contrast discrimination changes neuronal tuning and population coding in macaque V4. *Nature Communications*, 9(4238):1–15.

Sarabi, M. T., Aoki, R., Tsumura, K., Keerativittayayut, R., Jimura, K., and Nakahara, K. (2018). Visual perceptual training reconfigures post-task resting-state functional connectivity with a feature-representation region. *PLoS ONE*, 13(5):1–19.

Sasaki, Y., Nanez, J. E., and Watanabe, T. (2010). Advances in visual perceptual learning and plasticity. *Nature Reviews Neuroscience*, 11:53–60.

Schoups, A., Vogels, R., Qian, N., and Orban, G. (2001). Practising orientation identification improves orientation coding in V1 neurons. *Nature*, 412:549–553.

Schoups, A. A., Vogels, R., and Orban, G. A. (1995). Human perceptual learning in identifying the oblique orientation: retinotopy, orientation specificity and monocularity. *The Journal of Physiology*, 483(3):797–810.

Shadlen, M. N. and Newsome, W. T. (2001). Neural Basis of a Perceptual Decision in the Parietal Cortex (Area LIP) of the Rhesus Monkey. *Journal of Neurophysiology*, 86(4):1916–1936.

Shibata, K., Sagi, D., and Watanabe, T. (2014). Two-stage model in perceptual learning: toward a unified theory. *Annals of the New York Academy of Sciences*, 1316:18–28.

Shiozaki, H. M., Tanabe, S., Doi, T., and Fujita, I. (2012). Neural Activity in Cortical Area V4 Underlies Fine Disparity Discrimination. *Journal of Neuroscience*, 32(11):3830–3841.

Shohamy, D., Mihalakos, P., Chin, R., Thomas, B., Wagner, A. D., and Tamminga, C. (2010). Learning and generalization in schizophrenia: effects of disease and antipsychotic drug treatment. *Biological psychiatry*, 67(10):926–32.

Sotiropoulos, G., Seitz, A. R., and Seriès, P. (2018). Performance-monitoring integrated reweighting model of perceptual learning. *Vision Research*, 152:17–39.

Sowden, P. T., Davies, I. R. L., and Roling, P. (2000). Perceptual Learning of the Detection of Features in X-Ray Images: A Functional Role for Improvements in Adults' Visual Sensitivity? *Journal of Experimental Psychology: Human Perception and Performance*, 26(1):379–390.

Störmer, V. S., McDonald, J. J., and Hillyard, S. A. (2009). Cross-modal cueing of attention alters appearance and early cortical processing of visual stimuli. *Proceedings of the National Academy of Sciences*, 106(52):22456–22461.

Sun, L. D. and Goldberg, M. E. (2016). Corollary Discharge and Oculomotor Proprioception: Cortical Mechanisms for Spatially Accurate Vision. *Annual Review of Vision Science*, 2:61–84.

Talluri, B. C., Hung, S.-C., Seitz, A. R., and Seriès, P. (2015). Confidence-based integrated reweighting model of task-difficulty explains location-based specificity in perceptual learning. *Journal of Vision*, 15(10):17.

Tartaglia, E. M., Bamert, L., Herzog, M. H., and Mast, F. W. (2012). Perceptual learning of motion discrimination by mental imagery. *Journal of Vision*, 12(6):1–10.

Tartaglia, E. M., Bamert, L., Mast, F. W., and Herzog, M. H. (2009). Human Perceptual Learning by Mental Imagery. *Current Biology*, 19(24):2081–2085.

Tolias, A. S., Moore, T., Smirnakis, S. M., Tehovnik, E. J., Siapas, A. G., and Schiller, P. H. (2001). Eye movements modulate visual receptive fields of V4 neurons. *Neuron*, 29(3):757–767.

Treves, A. and Panzeri, S. (1995). The Upward Bias in Measures of Information Derived from Limited Data Samples. *Neural Computation*, 7(2):399–407.

Wang, L., Mruczek, R. E., Arcaro, M. J., and Kastner, S. (2015). Probabilistic maps of visual topography in human cortex. *Cerebral Cortex*, 25(10):3911–3931.

Wang, R., Zhang, J.-Y., Klein, S. a., Levi, D. M., and Yu, C. (2012). Task relevancy and demand modulate double-training enabled transfer of perceptual learning. *Vision research*, 61:33–38.

Wang, Z., Maier, A., Logothetis, N. K., and Liang, H. (2009). Extraction of Bistable-Percept-Related Features From Local Field Potential by Integration of Local Regression and Common Spatial Patterns. *IEEE Transactions on Biomedical Engineering*, 56(8):2095–2103.

Warren, S. G., Yacoub, E., and Ghose, G. M. (2014). Featural and temporal attention selectively enhance task-appropriate representations in human primary visual cortex. *Nature communications*, 5:5643.

Watanabe, T., Nanez, J. E., and Sasaki, Y. (2001). Perceptual learning without perception. *Nature*, 413:844–847.

Watanabe, T. and Sasaki, Y. (2015). Perceptual Learning: Toward a Comprehensive Theory. *Annual Review of Psychology*, 3(66):197–221.

Weiner, K. F. and Ghose, G. M. (2014). Rapid shape detection signals in area V4. *Frontiers in Neuroscience*, 8(294).

Weiner, K. F. and Ghose, G. M. (2015). Population coding in area V4 during rapid shape detections. *Journal of Neurophysiology*, 113(7):3021–3034.

Wenliang, L. and Seitz, A. R. (2018). Deep neural networks for modeling visual perceptual learning. *The Journal of Neuroscience*, 38(27):1620–17.

Wilke, M., Logothetis, N. K., and Leopold, D. A. (2006). Local field potential reflects perceptual suppression in monkey visual cortex. *Proceedings of the National Academy of Sciences*, 103(46):17507–17512.

Xiao, L.-Q., Zhang, J.-Y., Wang, R., Klein, S. a., Levi, D. M., and Yu, C. (2008). Complete transfer of perceptual learning across retinal locations enabled by double training. *Current biology*, 18:1922–1926.

Xie, X. Y. and Yu, C. (2018). Double training downshifts the threshold vs. noise contrast (TvC) functions with perceptual learning and transfer. *Vision Research*, 152:3–9.

Xing, D., Yeh, C.-I., and Shapley, R. M. (2009). Spatial Spread of the Local Field Potential and its Laminar Variation in Visual Cortex. *Journal of Neuroscience*, 29(37):11540–11549.

Y, Y. and M, C. (1999). Spatial attention improves performance in spatial resolution tasks. *Vision Research*, 39(2):293–306.

Yan, Y., Rasch, M. J., Chen, M., Xiang, X., Huang, M., Wu, S., and Li, W. (2014). Perceptual training continuously refines neuronal population codes in primary visual cortex. *Nature Neuroscience*, 17(10):1380–1387.

Yang, T. and Maunsell, J. H. R. (2004). The effect of perceptual learning on neuronal responses in monkey visual area V4. *The Journal of neuroscience : the official journal of the Society for Neuroscience*, 24(7):1617–26.

Yeshurun, Y. and Carrasco, M. (1998). Attention improves or impairs visual performance by enhancing spatial resolution. *Nature*, 396(6706):1–8.

Yeshurun, Y., Montagna, B., and Carrasco, M. (2008). On the flexibility of sustained attention and its effects on a texture segmentation task. *Vision Research*, 48(1):80–95.

Zaidel, A., Deangelis, G. C., and Angelaki, D. E. (2017). Decoupled choice-driven and stimulus-related activity in parietal neurons may be misrepresented by choice probabilities. *Nature Communications*, 8(1).

Zhang, J., Meeson, A., Welchman, A. E., and Kourtzi, Z. (2010a). Learning alters the tuning of functional magnetic resonance imaging patterns for visual forms. *The Journal of neuroscience : the official journal of the Society for Neuroscience*, 30(42):14127–14133.

Zhang, J.-Y., Zhang, G.-L., Xiao, L.-Q., Klein, S. a., Levi, D. M., and Yu, C. (2010b). Rule-based learning explains visual perceptual learning and its specificity and transfer. *The Journal of Neuroscience*, 30(37):12323–12328.

Zhang, T., Xiao, L.-Q., Klein, S. a., Levi, D. M., and Yu, C. (2010c). Decoupling location specificity from perceptual learning of orientation discrimination. *Vision research*, 50:368–374.

Zuanazzi, A. and Noppeney, U. (2019). Distinct neural mechanisms of spatial attention and expectation guide perceptual inference in a multisensory world Distinct neural mechanisms of spatial attention and expectation guide perceptual inference in a multisensory world Abbreviated title : Multi. *Journal of Neuroscience*, 39(12):2301–2312.

Zuo, Y., Safaai, H., Notaro, G., Mazzoni, A., Panzeri, S., and Diamond, M. E. (2015). Complementary contributions of spike timing and spike rate to perceptual decisions in rat S1 and S2 cortex. *Current Biology*, 25(3):357–363.